The First Direct Observation of a Gravitational Wave Signal

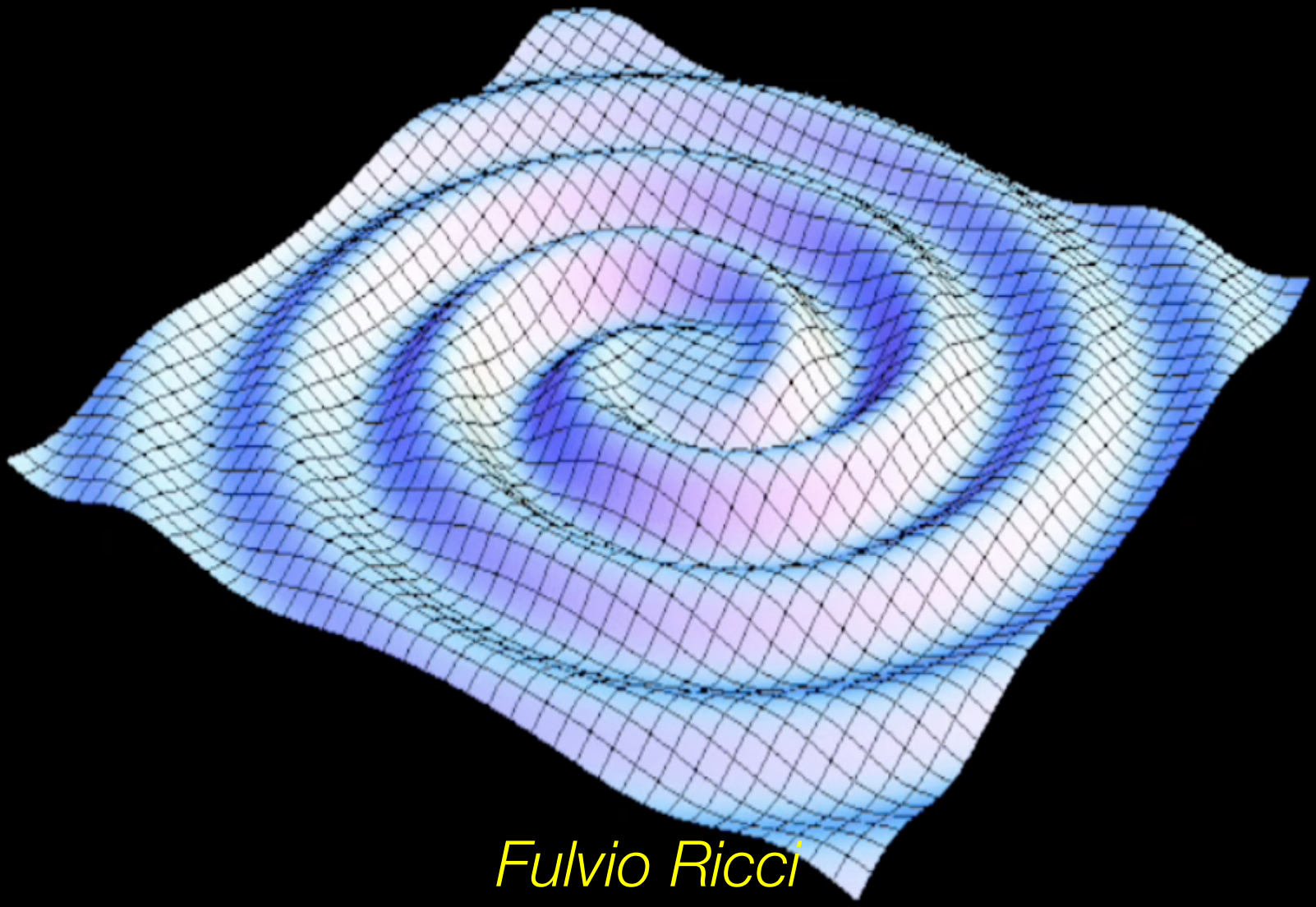

Fulvio Ricci
Università di Roma Sapienza & INFN - Sezione di Roma

General Relativity

1916

Die Feldgleichungen der Gravitation.

Von A. Einstein.

In zwei vor kurzem erschienenen Mitteilungen[1] habe ich gezeigt, wie man zu Feldgleichungen der Gravitation gelangen kann, die dem Postulat allgemeiner Relativität entsprechen, d. h. die in ihrer allgemeinen Fassung beliebigen Substitutionen der Raumzeitvariabeln gegenüber kovariant sind.

Der Entwicklungsgang war dabei folgender. Zunächst fand ich Gleichungen, welche die Newtonsche Theorie als Näherung enthalten und beliebigen Substitutionen von der Determinante 1 gegenüber kovariant waren. Hierauf fand ich, daß diesen Gleichungen allgemein kovariante entsprechen, falls der Skalar des Energietensors der »Materie« verschwindet. Das Koordinatensystem war dann nach der einfachen Regel zu spezialisieren, daß $\sqrt{-g}$ zu 1 gemacht wird, wodurch die Gleichungen der Theorie eine eminente Vereinfachung erfahren. Dabei mußte aber, wie erwähnt, die Hypothese eingeführt werden, daß der Skalar des Energietensors der Materie verschwinde.

Neuerdings finde ich nun, daß man ohne Hypothese über den Energietensor der Materie auskommen kann, wenn man den Energietensor der Materie in etwas anderer Weise in die Feldgleichungen einsetzt, als dies in meinen beiden früheren Mitteilungen geschehen ist. Die Feldgleichungen für das Vakuum, auf welche ich die Erklärung der Perihelbewegung des Merkur gegründet habe, bleiben von dieser Modifikation unberührt. Ich gebe hier nochmals die ganze Betrachtung, damit der Leser nicht genötigt ist, die früheren Mitteilungen unausgesetzt heranzuziehen.

Aus der bekannten Riemannschen Kovariante vierten Ranges leitet man folgende Kovariante zweiten Ranges ab:

$$G_{im} = R_{im} + S_{im} \tag{1}$$

$$R_{im} = -\sum_l \frac{\partial \left\{ \begin{matrix} im \\ l \end{matrix} \right\}}{\partial x_l} + \sum_{lz} \left\{ \begin{matrix} il \\ z \end{matrix} \right\} \left\{ \begin{matrix} mz \\ l \end{matrix} \right\} \tag{1a}$$

$$S_{im} = \sum_l \frac{\partial \left\{ \begin{matrix} il \\ l \end{matrix} \right\}}{\partial x_m} - \sum_{lz} \left\{ \begin{matrix} im \\ z \end{matrix} \right\} \left\{ \begin{matrix} zl \\ l \end{matrix} \right\} \tag{1b}$$

[1] Sitzungsber. XLIV. S. 778 und XLVI. S. 799. 1915.

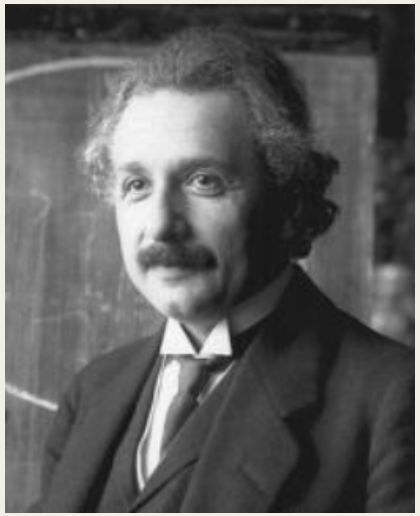

1918

Über Gravitationswellen.

Von A. Einstein.

Die wichtige Frage, wie die Ausbreitung der Gravitationsfelder erfolgt, ist schon vor anderthalb Jahren in einer Akademiearbeit von mir behandelt worden[1]. Da aber meine damalige Darstellung des Gegenstandes nicht genügend durchsichtig und außerdem durch einen bedauerlichen Rechenfehler verunstaltet ist, muß ich hier nochmals auf die Angelegenheit zurückkommen.

Wie damals beschränke ich mich auch hier auf den Fall, daß las betrachtete zeiträumliche Kontinuum sich von einem »galileischen« nur sehr wenig unterscheidet. Um für alle Indizes

$$g_{\mu\nu} = -\delta_{\mu\nu} + \gamma_{\mu\nu} \tag{1}$$

setzen zu können, wählen wir, wie es in der speziellen Relativitätstheorie üblich ist, die Zeitvariable x_4 rein imaginär, indem wir

$$x_4 = it$$

setzen, wobei t die »Lichtzeit« bedeutet. In (1) ist $\delta_{\mu\nu} = 1$ bzw. $\delta_{\mu\nu} = 0$, je nachdem $\mu = \nu$ oder $\mu \neq \nu$ ist. Die $\gamma_{\mu\nu}$ sind gegen 1 kleine Größen, welche die Abweichung des Kontinuums vom feldfreien darstellen; sie bilden einen Tensor vom zweiten Range gegenüber Lorentz-Transformationen.

§ 1. Lösung der Näherungsgleichungen des Gravitationsfeldes durch retardierte Potentiale.

Wir gehen aus von den für ein beliebiges Koordinatensystem gültigen[2] Feldgleichungen

$$-\sum_\alpha \frac{\partial}{\partial x_\alpha} \left\{ \begin{matrix} \mu\nu \\ \alpha \end{matrix} \right\} + \sum_\alpha \frac{\partial}{\partial x_\nu} \left\{ \begin{matrix} \mu\alpha \\ \alpha \end{matrix} \right\} + \sum_{\alpha\beta} \left\{ \begin{matrix} \mu\alpha \\ \beta \end{matrix} \right\} \left\{ \begin{matrix} \nu\beta \\ \alpha \end{matrix} \right\} - \sum_{\alpha\beta} \left\{ \begin{matrix} \mu\nu \\ \alpha \end{matrix} \right\} \left\{ \begin{matrix} \alpha\beta \\ \beta \end{matrix} \right\} = -\varkappa \left(T_{\mu\nu} - \frac{1}{2} g_{\mu\nu} T \right). \tag{2}$$

[1] Diese Sitzungsber. 1916, S. 688 ff.

[2] Von der Einführung des »λ-Gliedes« (vgl. diese Sitzungsber. 1917, S. 142) ist dabei Abstand genommen.

Experimental Gravitational

- GR verifications in the ***weak field regime:***
  - Precession of Mercury's perihelion,
  - Gravitational lensing and Shapiro delay and in generle Solar System tests as those setting upper limits of graviton mass, measure Lens Thirring effect by Lageos/Lares and Garvity probe B
- Astronomical observation based on binary systems:
  - PSR B1913+16 confirmed the expected cumulative energy loss measured through pulsar spindown

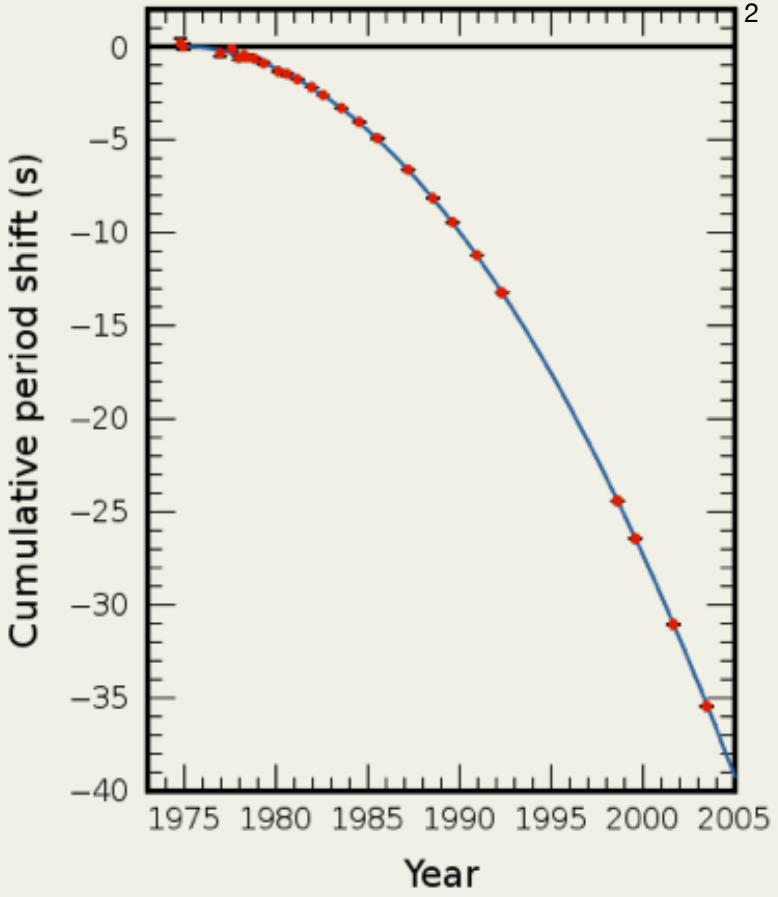

Gravitation and Gravitational Waves

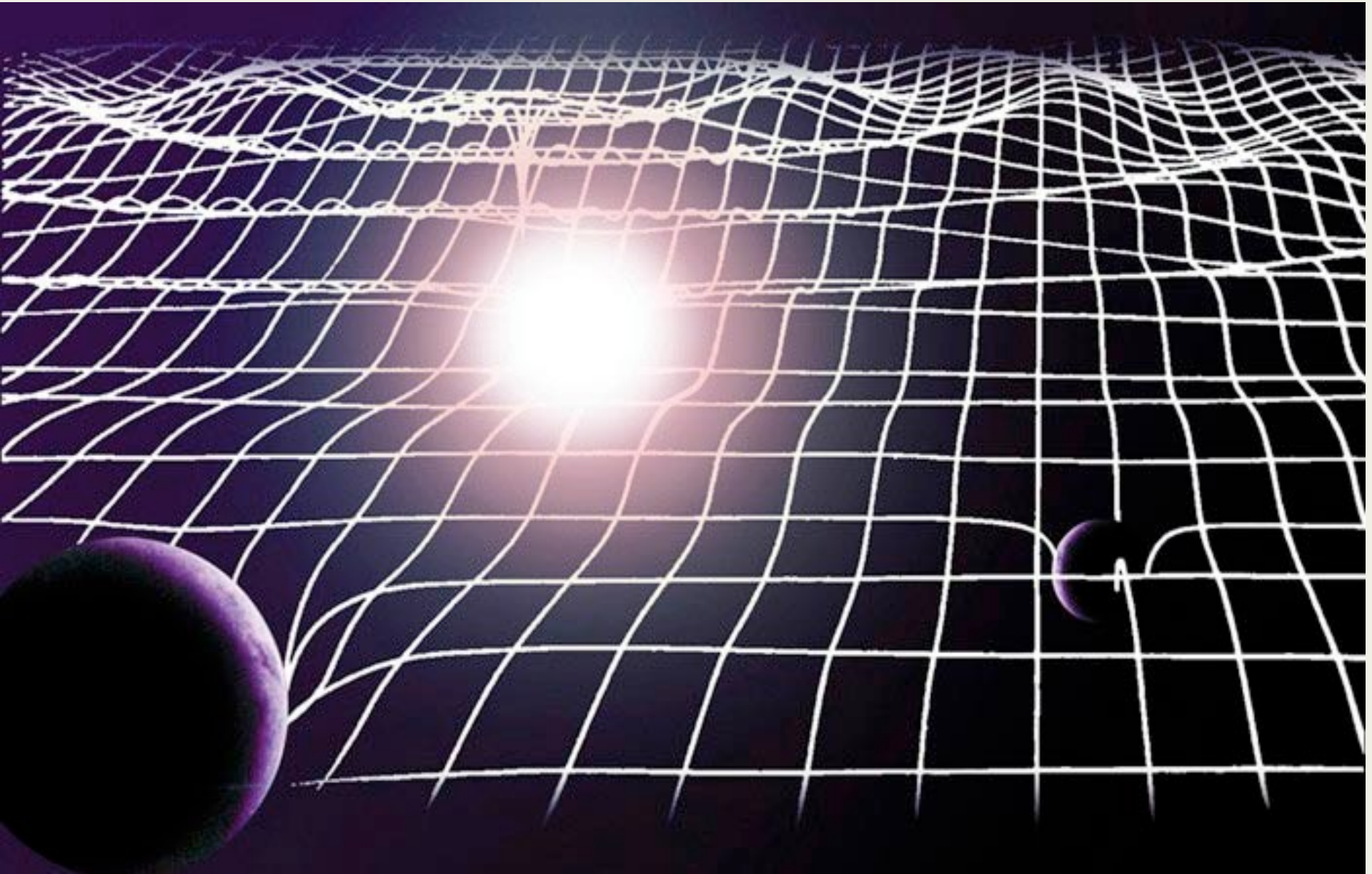

The detection principle

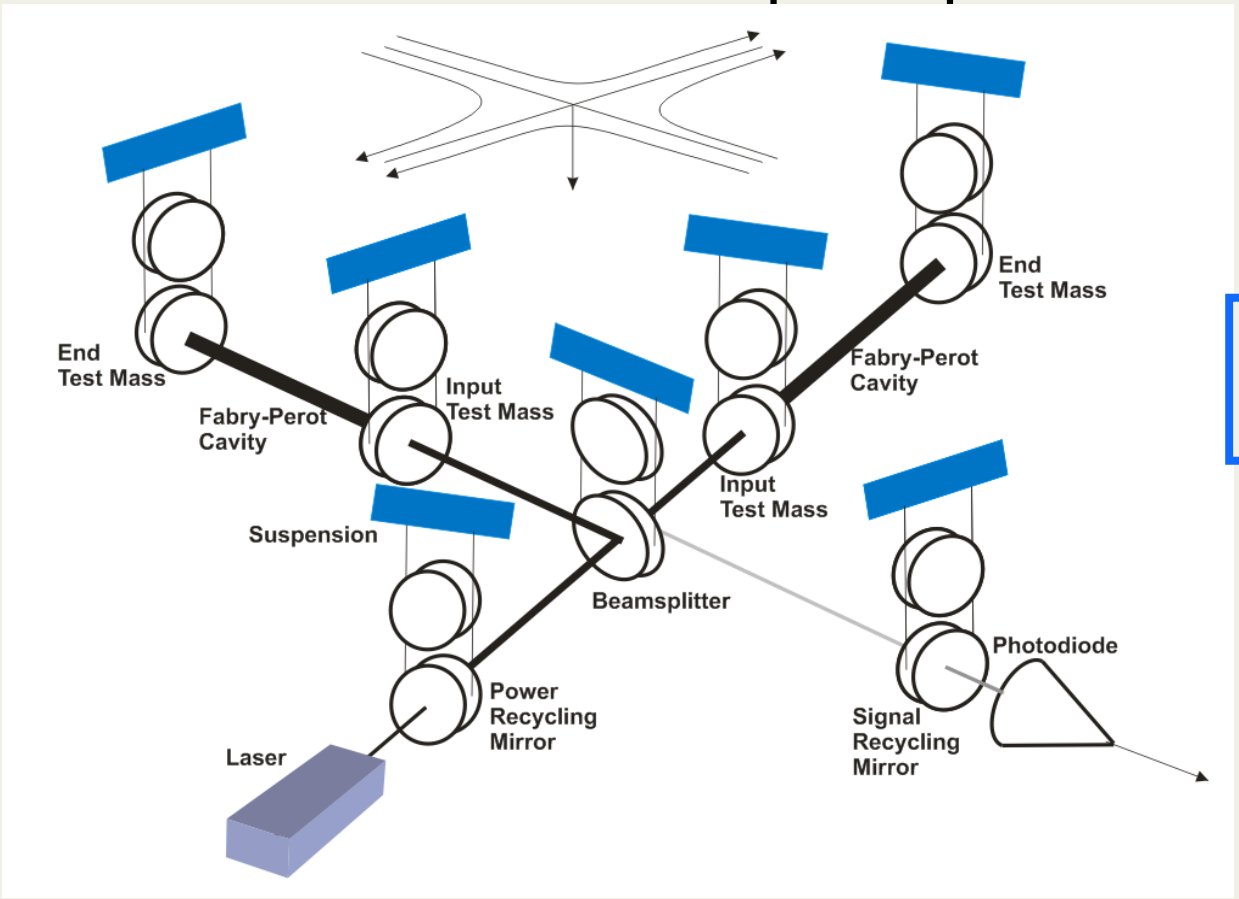

$$h = \frac{\Delta L}{L} \sim 10^{-22}$$

$$i_{pd}(t) = \frac{\Delta L}{L}(t)$$

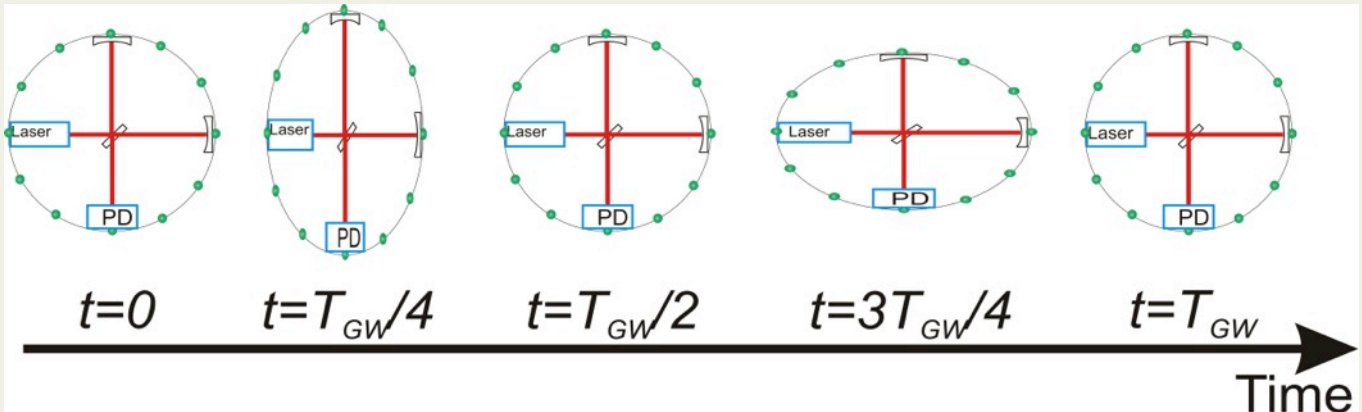

Location in the sky

- GW laser interferometers are not pointing telescopes,

- Sky location can be reconstructed through the time of arrival of GW radiation at the different detector sites, as well as the relative amplitude and phase of the GWs in different detectors.

Antenna pattern

F_+ 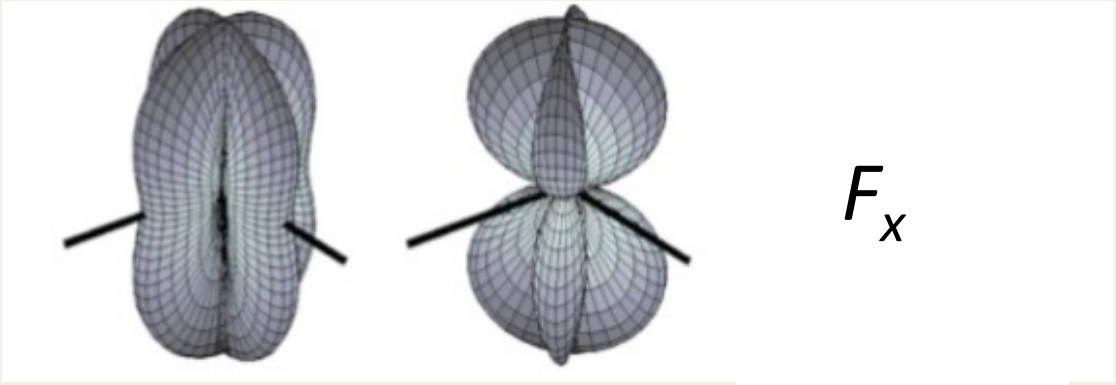 F_x

$$h = F_+(\alpha, \delta, \psi)\, h_+ + F_-(\alpha, \delta, \psi)\, h_-$$

Sky position and polarization angle

- The radiation emitted in a CBC along the orbital axis ➔ circularly polarized
- The radiation emitted in a CBC on the equatorial plane ➔ linearly polarized

- Observing with more than one detector we can infer both the location in the sky and the degree of elliptical polarization

- The accuracy on position and polarization depends on the accuracy of amplitude and arrival time of the signal

Transient Source Localization: 2 detectors

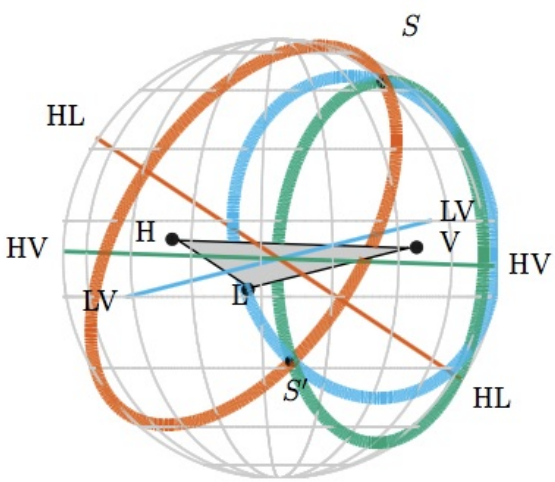

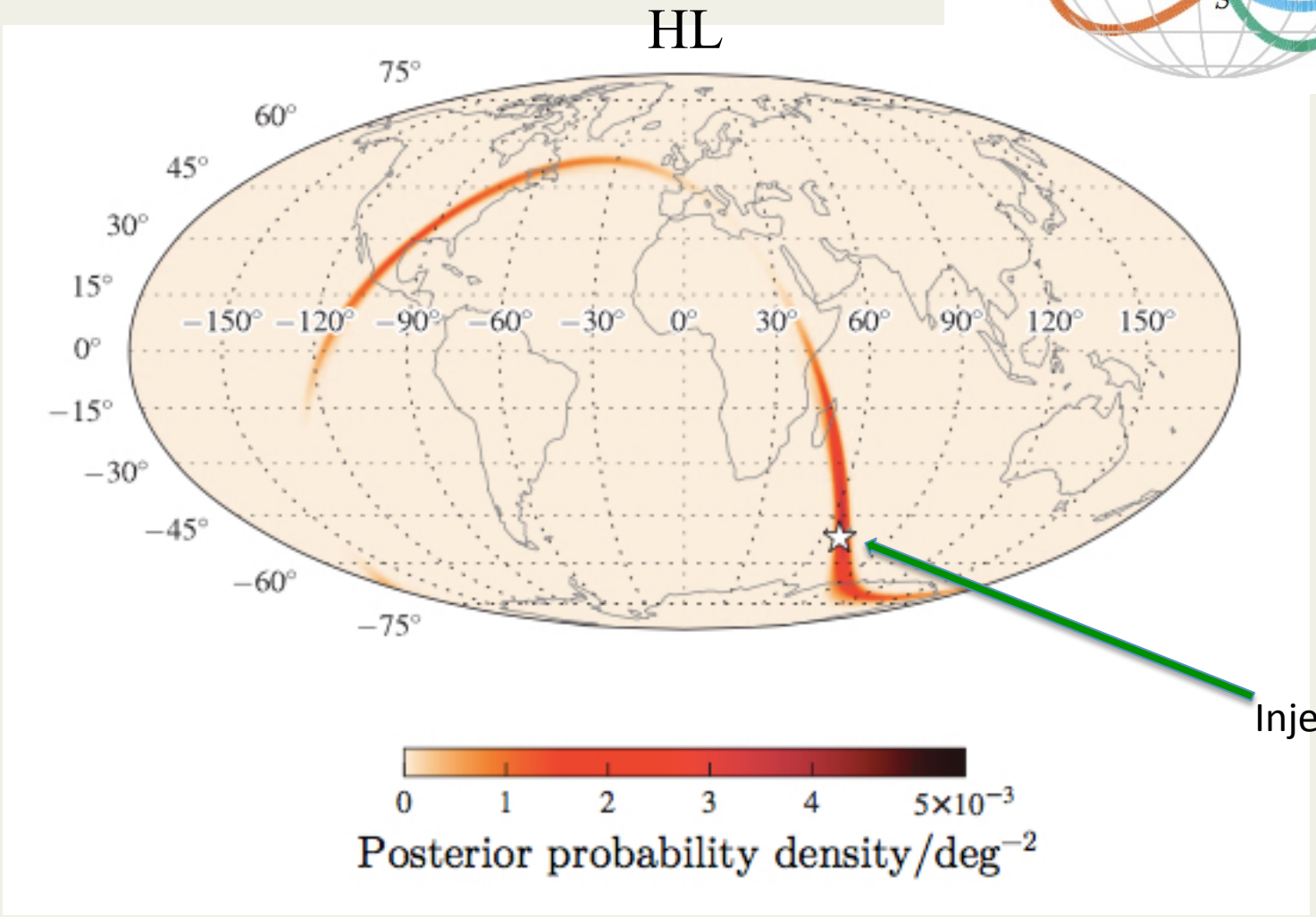

Transient Source Localization: 3 , 4 , 5 detectors

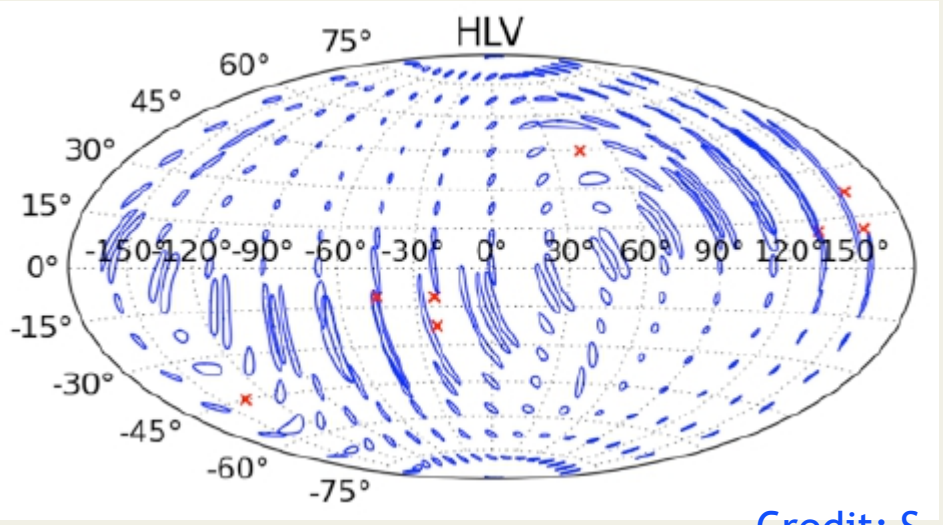

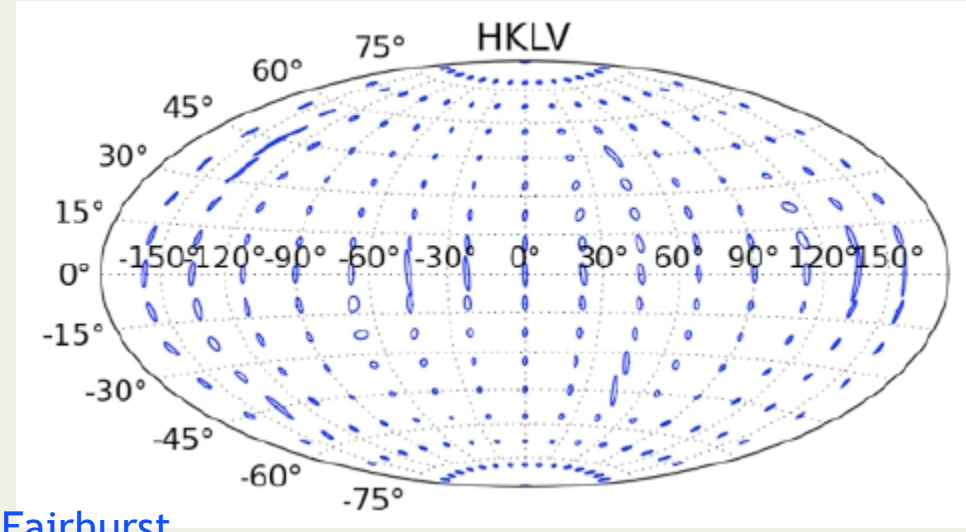

Credit: S. Fairhurst

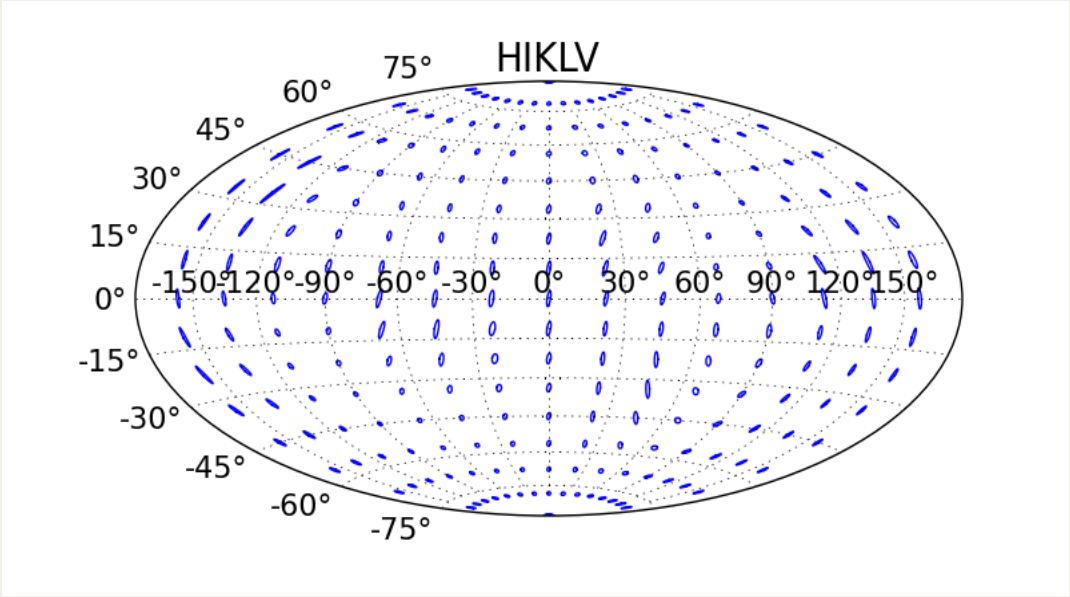

The 2007 GW network

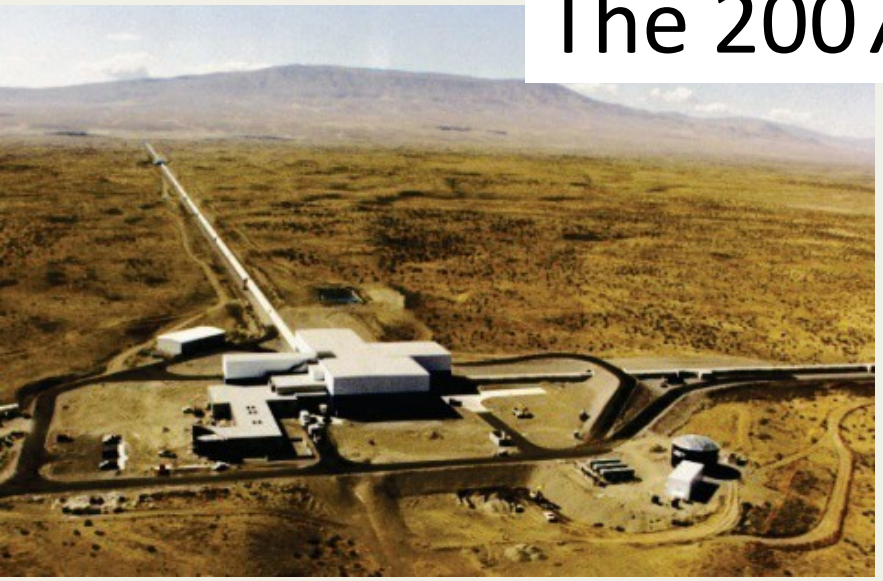

H1- Hanford – Washington state

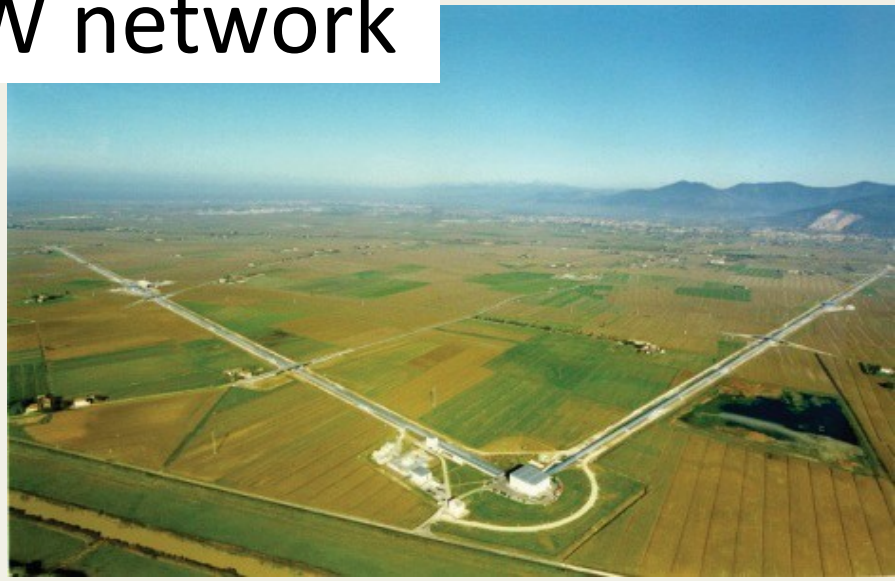

Virgo – Cascina (Pisa) – EGO site

GEO600 – Hannover - Germany

L1- Livingston – Louisiana state

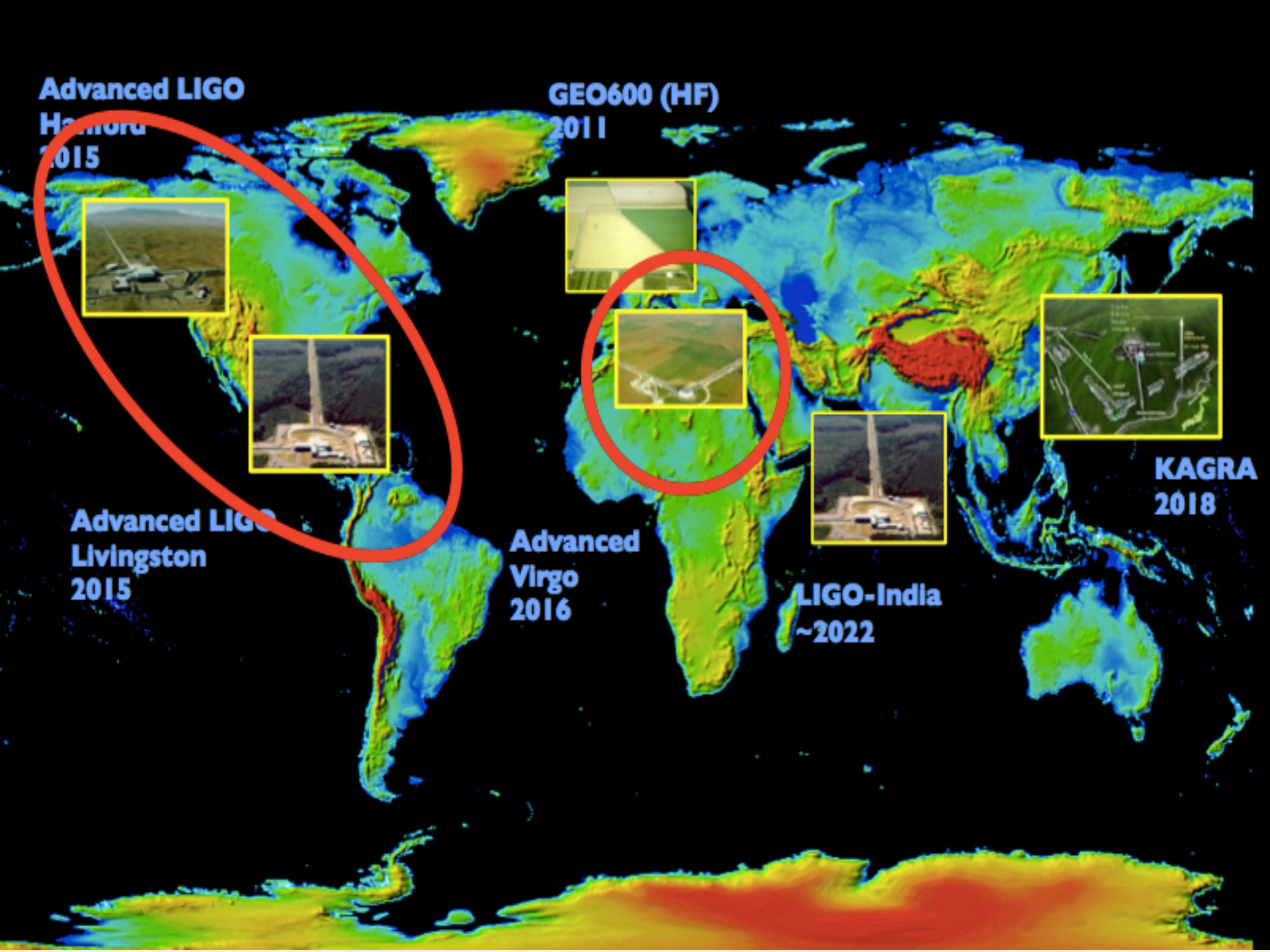
Advanced LIGO
Hanford
2015
GEO600 (HF)
2011
Advanced LIGO
Livingston
2015
Advanced
Virgo
2016
LIGO-India
~2022
KAGRA
2018

H1- Hanford – Washington state

LIGO upgrade concluded

The Advanced LIGO dedication ceremony was held at Hanford on May 19, 2015

VIRGO will end the upgrade in 2016

L1- Livingston – Louisiana state

The first month of the run

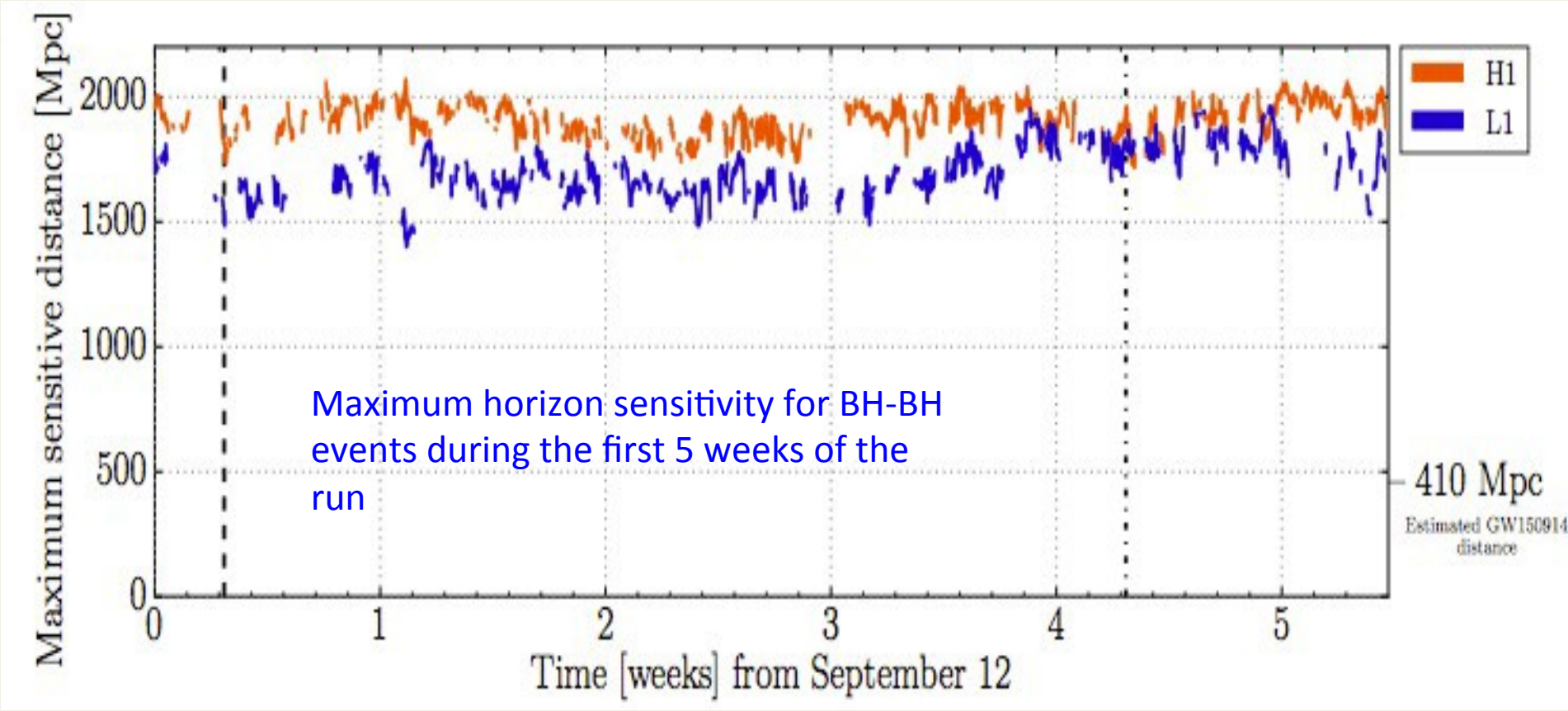

- Interferometers locked in their nominal data-taking configurations
  - The performance of the instruments **exceeded** the median expected, and almost met the upper range expected in the 2015 (O1) observation run

How the signal might look like

This source:

Embedded in this noise

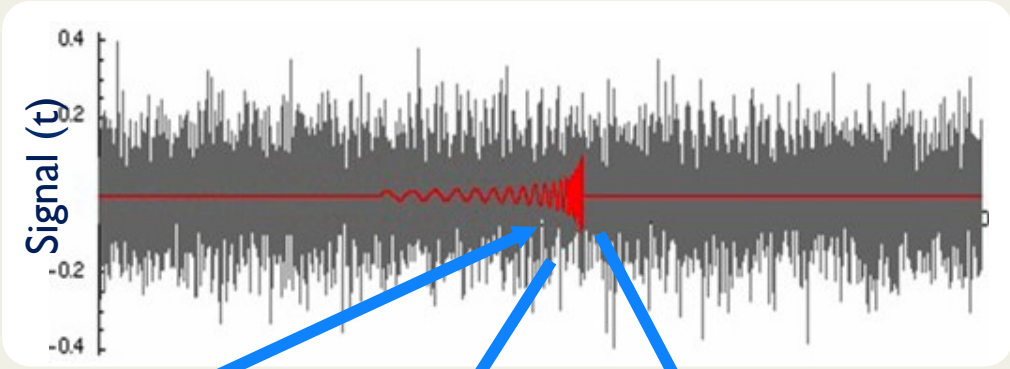

Produces this waveform:

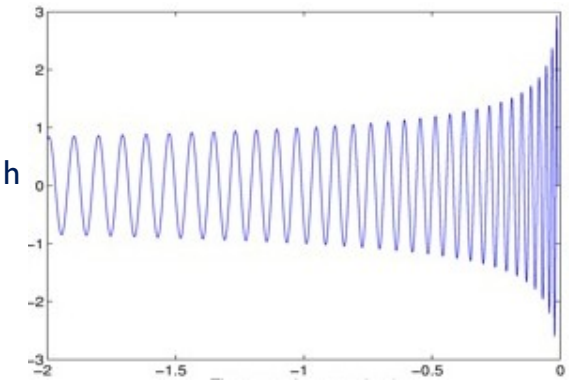

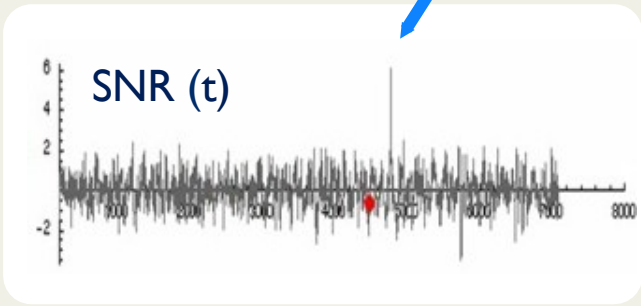

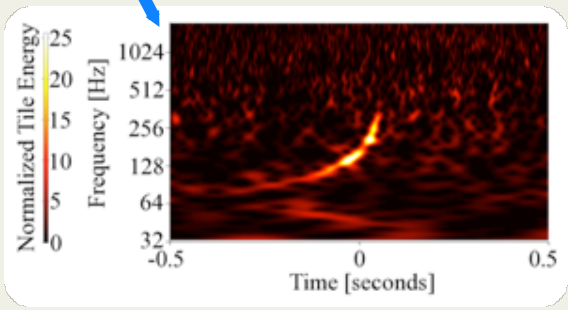

matched filtering or excess power

Coherent Wave Burst (cWB) algorithm: minimal assumption for searching transients

- Require coherent signals in multiple detectors, using direction-dependent antenna response

- Look for excess power in time-frequency space using wavelet decomposition

The event are ranked using a variable quoting
the SNR of the coherent signal in the network

$$\eta_c = \sqrt{\frac{2E_c}{(1 + E_n/E_c)}}$$

E_c ➔ Normalized coherent energy between the two detectors

E_n ➔ normalized noise energy derived by subtracting the reconstructed signal from the data

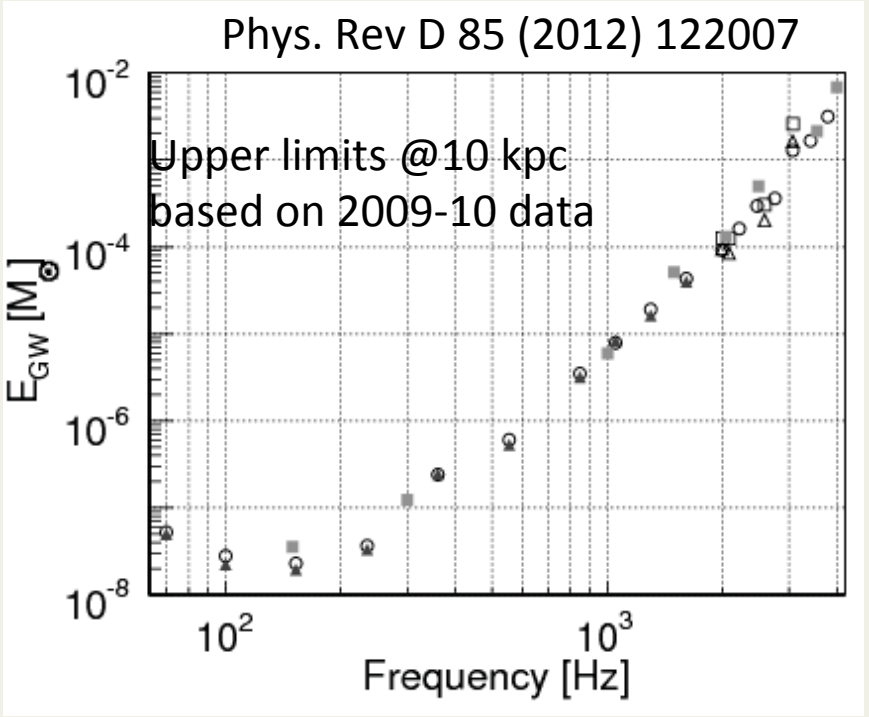

A Golden GW Signal

Compact Binary Coalescence

- Time dependent quadrupole moment
  - CBC emit gravitational radiation:

    $P_{GW} \sim M^3/r^5$,
- Strong field general relativity takes over at some point.
  - Over the last stable orbits, they merge, forming a single compact object

	Earth + Sun	$1.4\ M_\odot$ + $1.4\ M_\odot$
P_{GW}	$\sim 10^2$ W	$\sim 10^{48}$ W
(df/dt) * (1/f)	10^{-33} Hz	10^2 Hz

System Parameterization

At a given reference time t_c / assume zero eccentricity

Extrinsic

Intrinsic

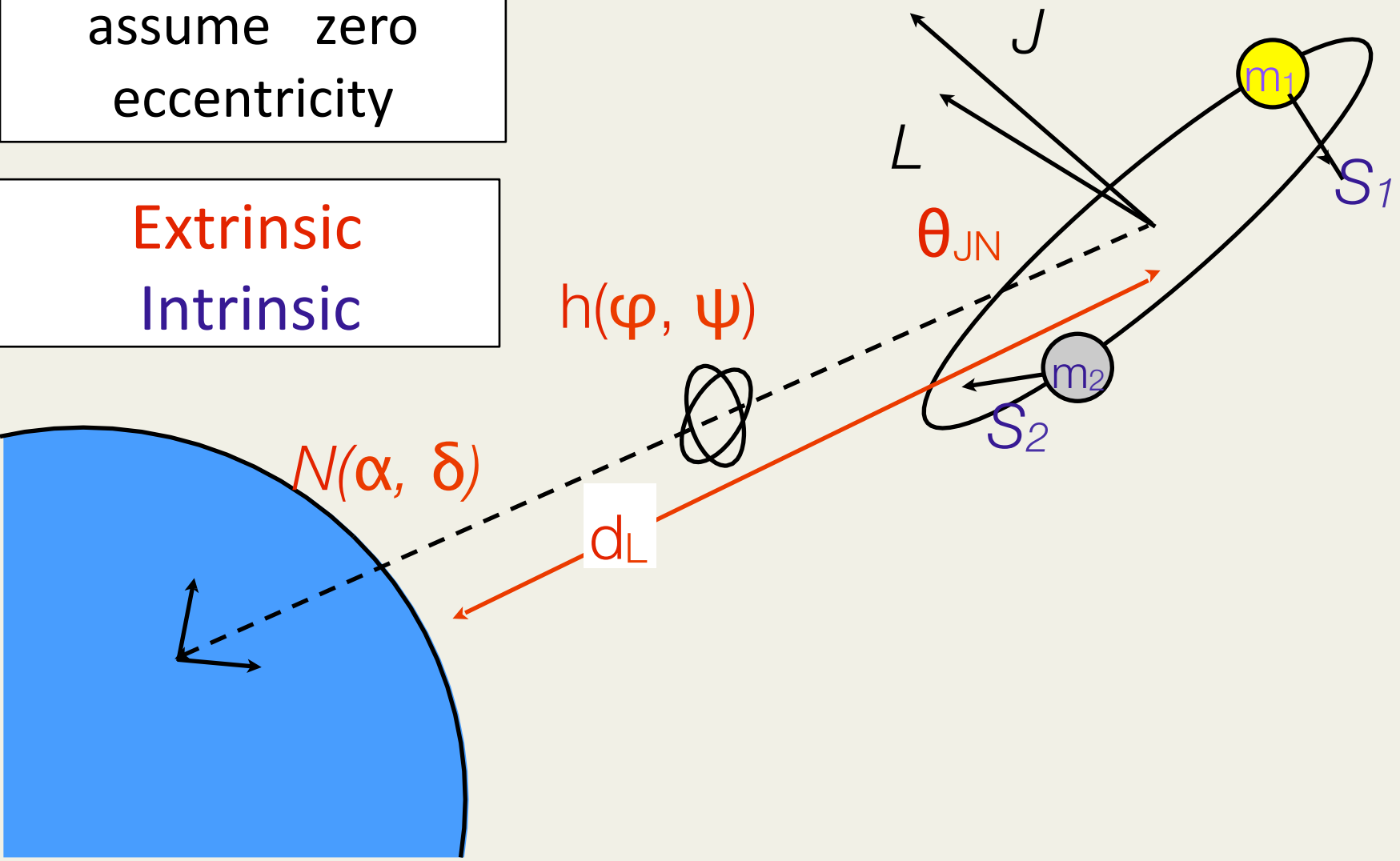

Compact Binary Coalescence: Waveforms

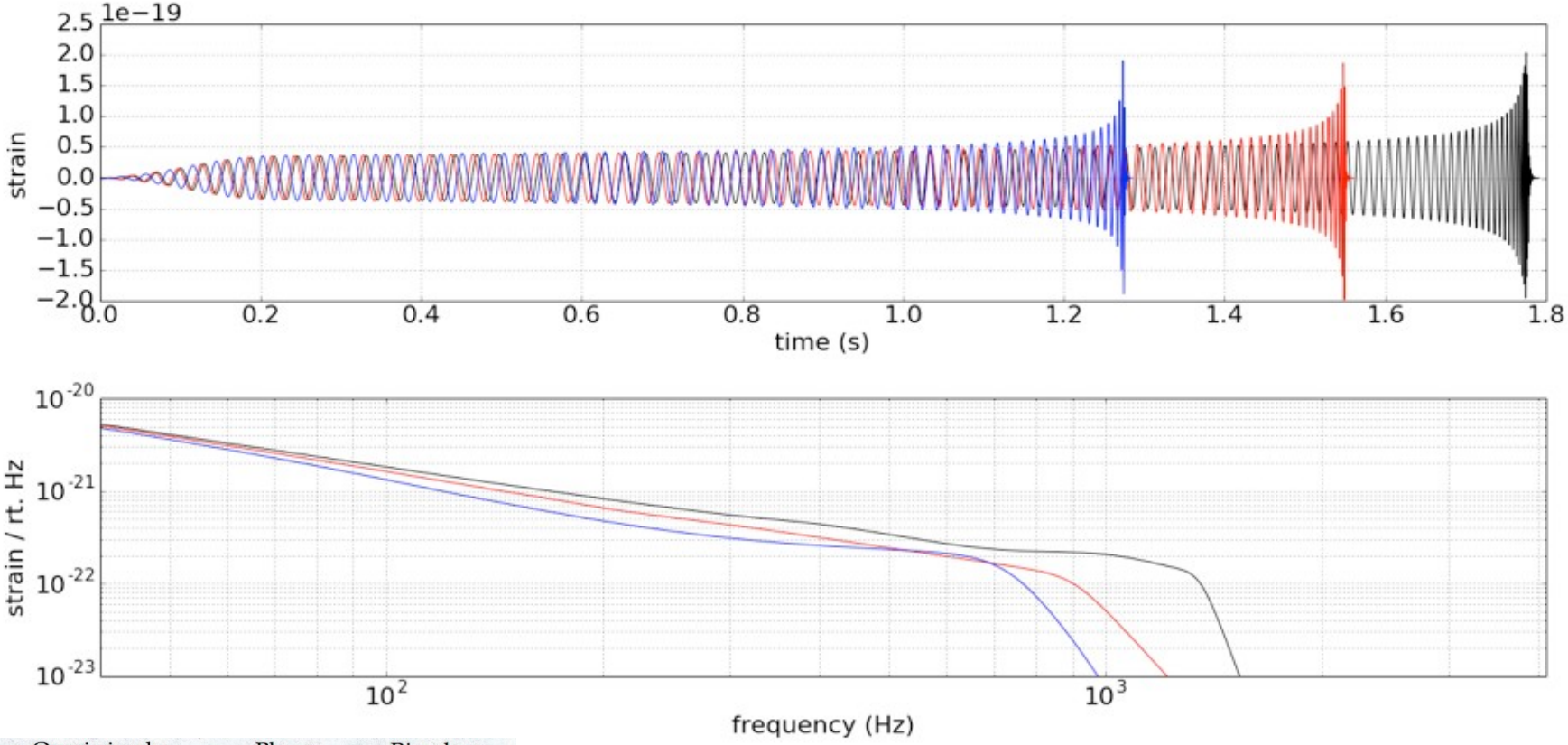

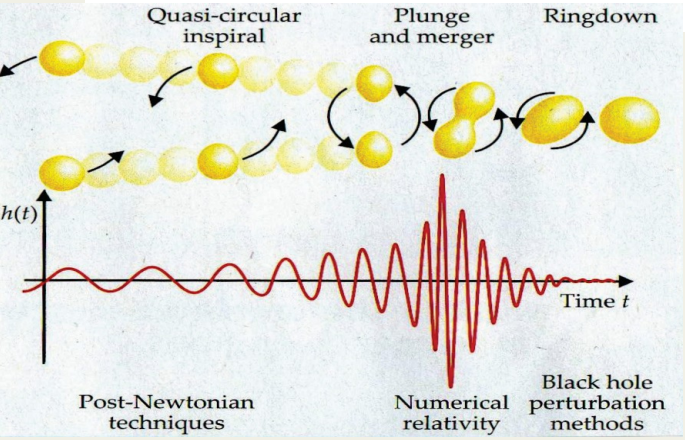

$m_1 = m_2 = 10\ M_\odot$

$s_{1,z} = s_{2,z} = 0.99$ $s_{1,z} = 0.99,\ s_{2,z} = -0.99$

$s_{1,z} = s_{2,z} = -0.99$

Compact Binary Coalescence: Waveforms

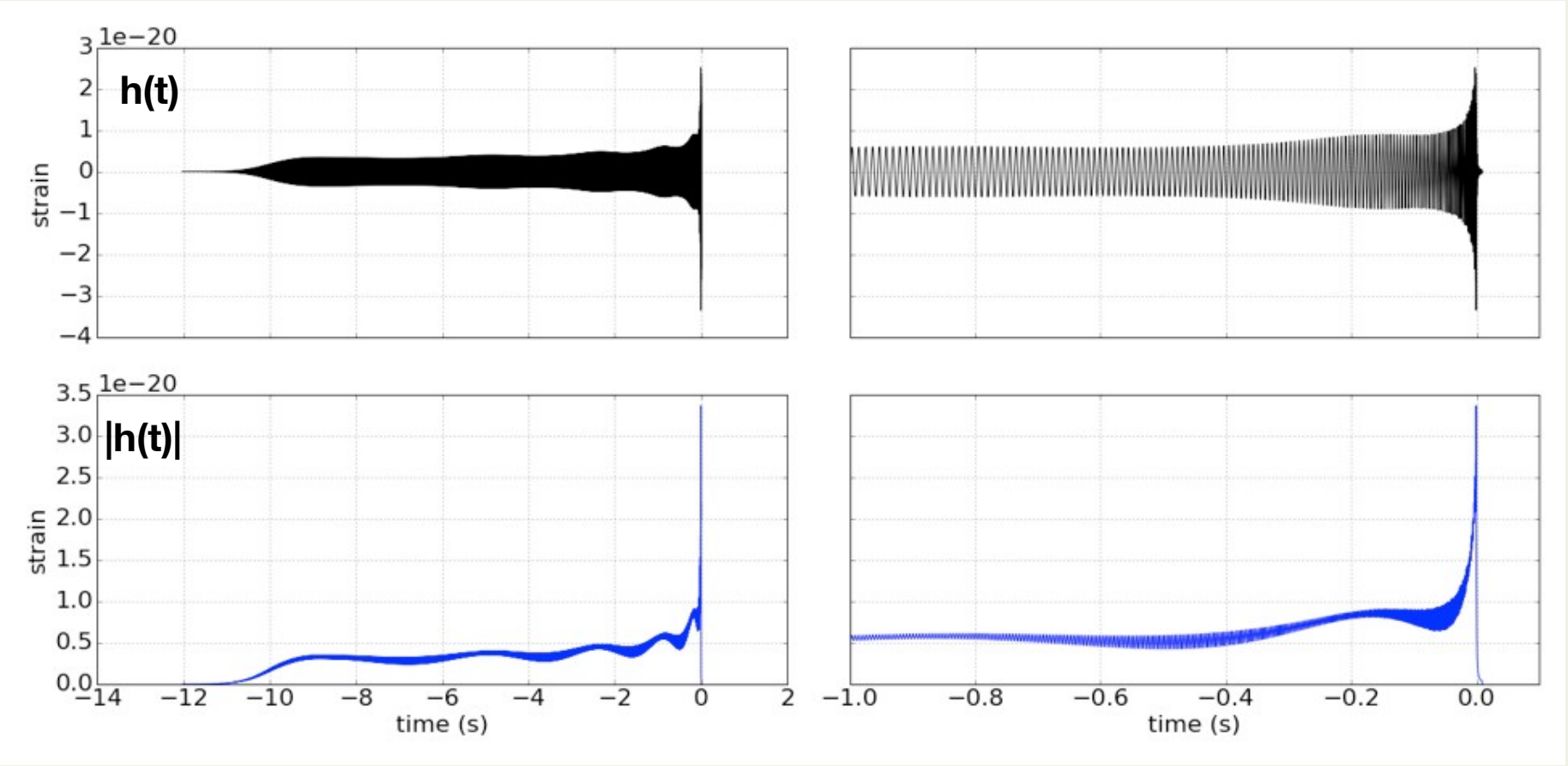

Effects of Precession $m_1 = 5$ $m_2 = 1.4$

$s_{1,x} = s_{1,y} = 0.5$

modulation envelope

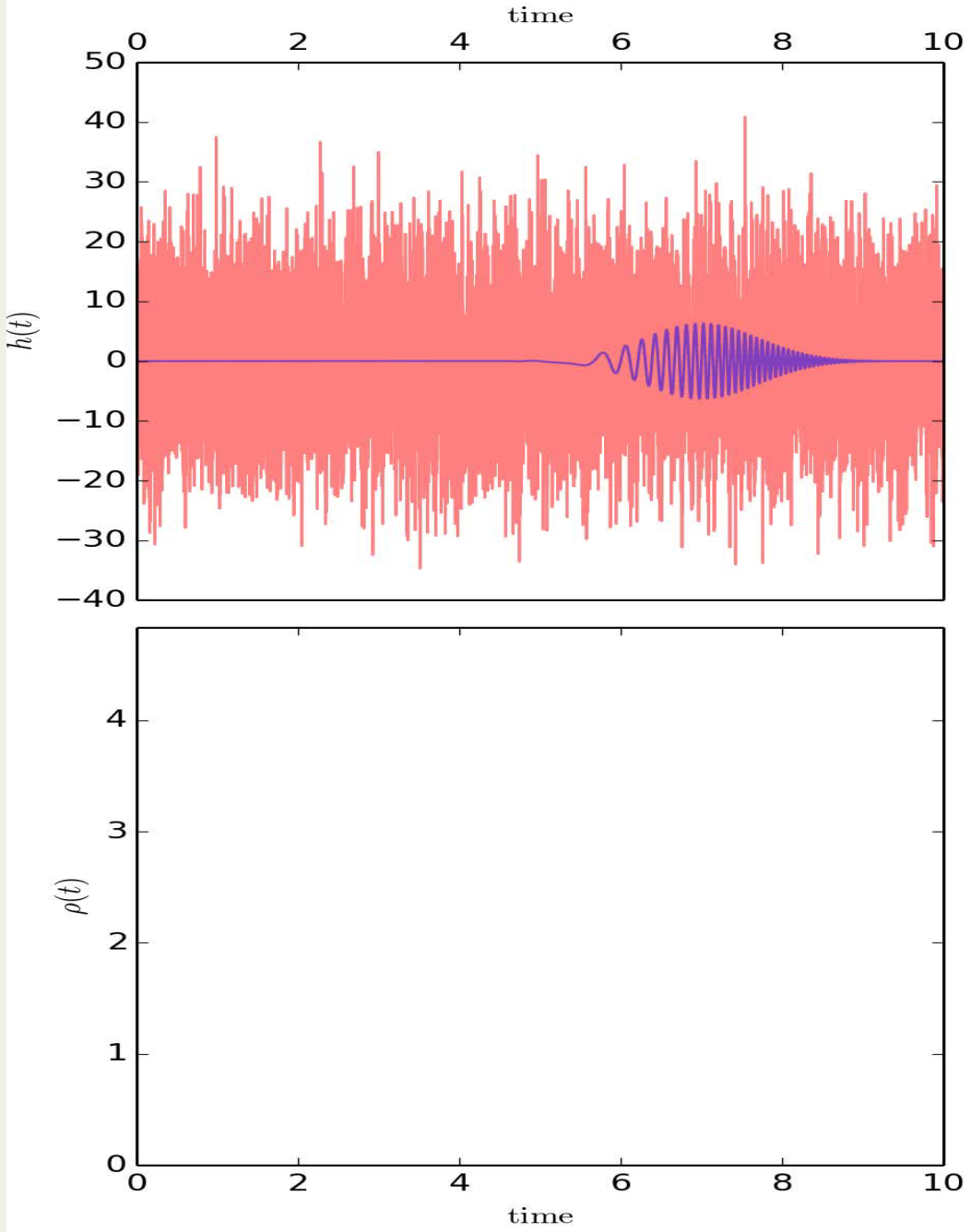

Assuming that the signal is CBC like: matched filter search

Waveform consistency test: χ^2 test

- Divide the "selected" template into p parts
- The frequency intervals are chosen so that for a true signal, the SNR is uniformly shared among the frequency bands
- For a stationary and Gaussian noise has an expectation value:

$$\chi^2(t) = p\sum_{j=1}^{p} |\rho_j - \frac{\rho}{p}|^2$$

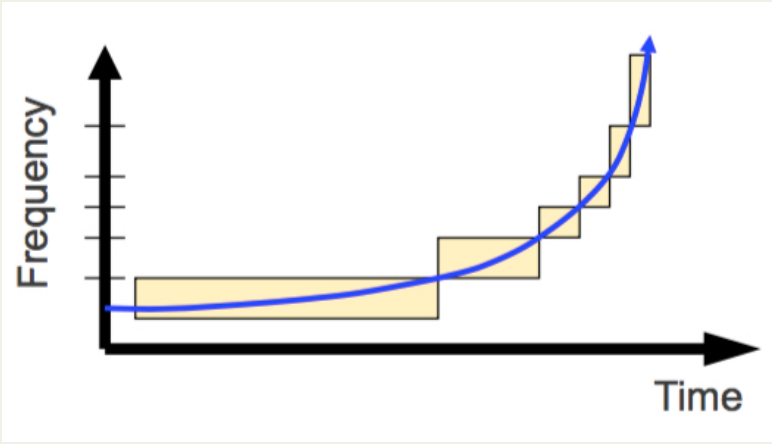

- In practise χ^2 values are larger than expected for large SNR (discrete template banks effect) → cut in (SNR, χ^2) plane
- Weighted SNR

$$\rho_{\text{new}} = \begin{cases} \rho, & \chi^2 \leq n_{\text{dof}} \\ \dfrac{\rho}{\left[\left(1 + \frac{\chi^2}{n_{dof}}^{4/3}\right)/2\right]^{1/4}}, & \chi^2 > n_{\text{dof}} \end{cases}$$

χ^2

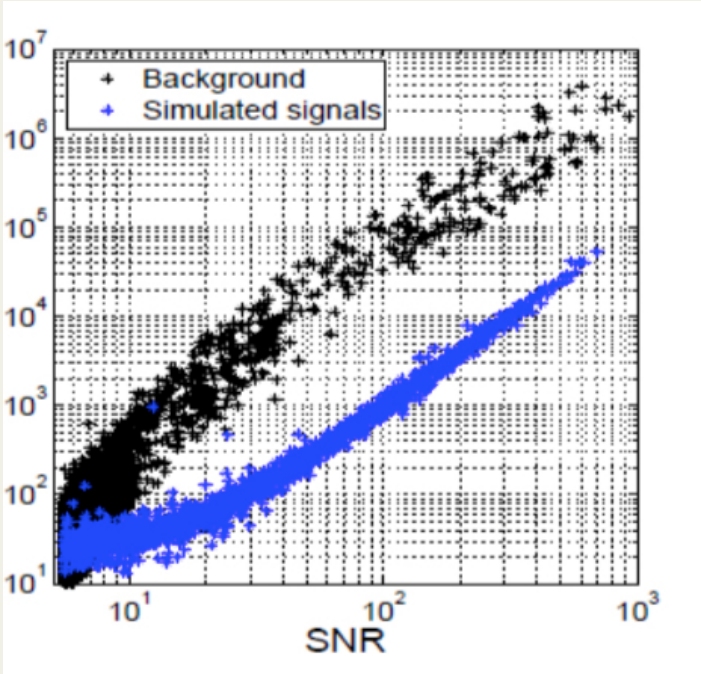

Background estimation

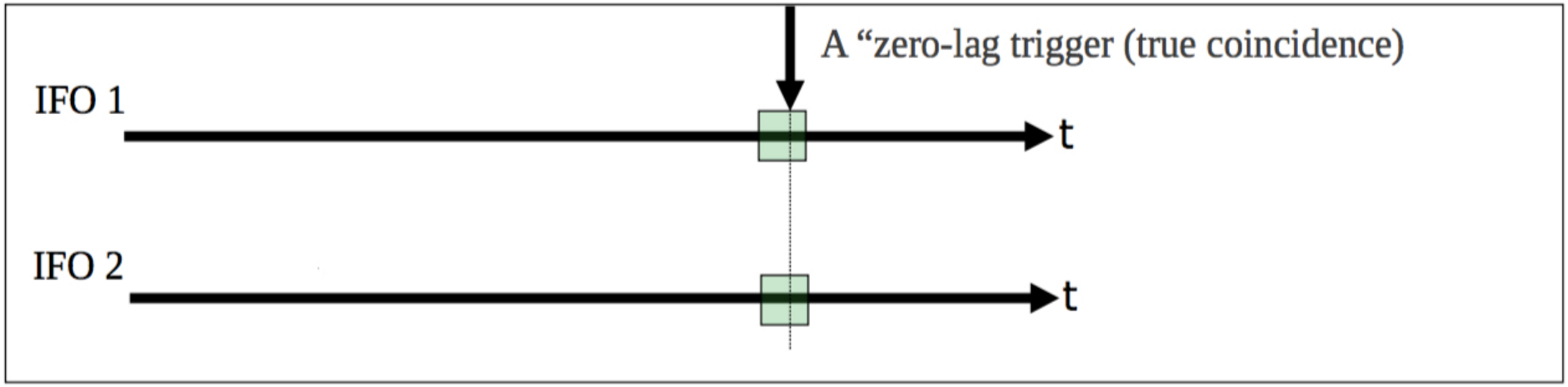

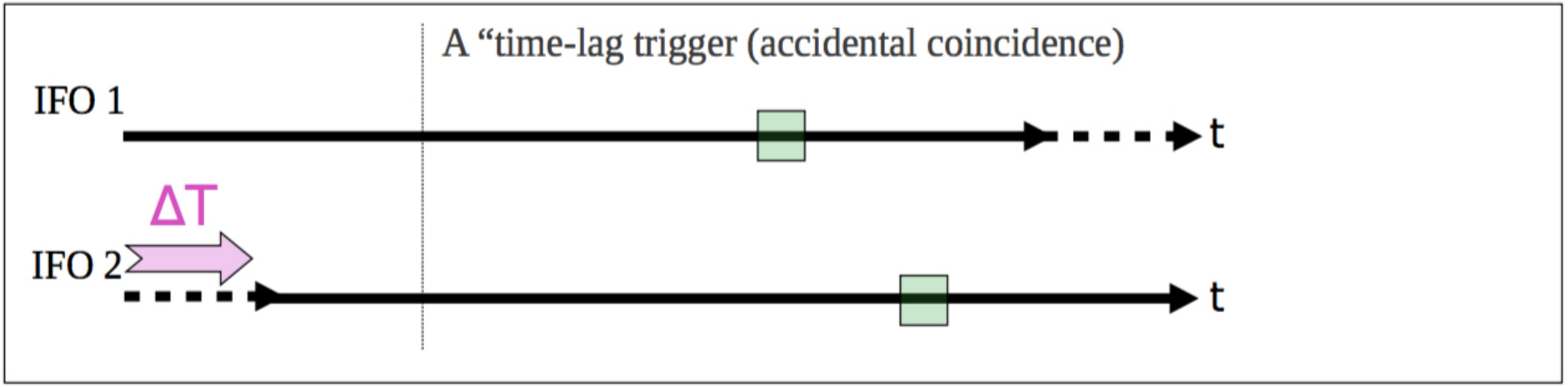

The First Month of Observation Run 1

- The analysis covered the period from September 12th to October 20th

- 16 days of coincidence data (both Hanford and Livingston locked)

Potential horizon for different kind of CCB signals

- 1.4 $M_\odot$ + 1.4 $M_\odot$ ➔horizon: 130 Mpc
- 1.4 $M_\odot$ + 5 $M_\odot$ ➔horizon: 200 Mpc
- 20 $M_\odot$ + 20$M_\odot$ ➔ horizon: ~1 Gpc

Signal-to-Noise ratio (SNR)

$$\rho = 4 \int_0^\infty \frac{\tilde{h}(f)\tilde{d}(f)^*}{S(f)} df$$

Horizon distance (luminosity)

$$d_h = \frac{4}{\bar{\rho}} \int_0^\infty \frac{\tilde{h}_{1\ \mathrm{Mpc}}(f)\tilde{d}(f)^*}{S(f)} df$$

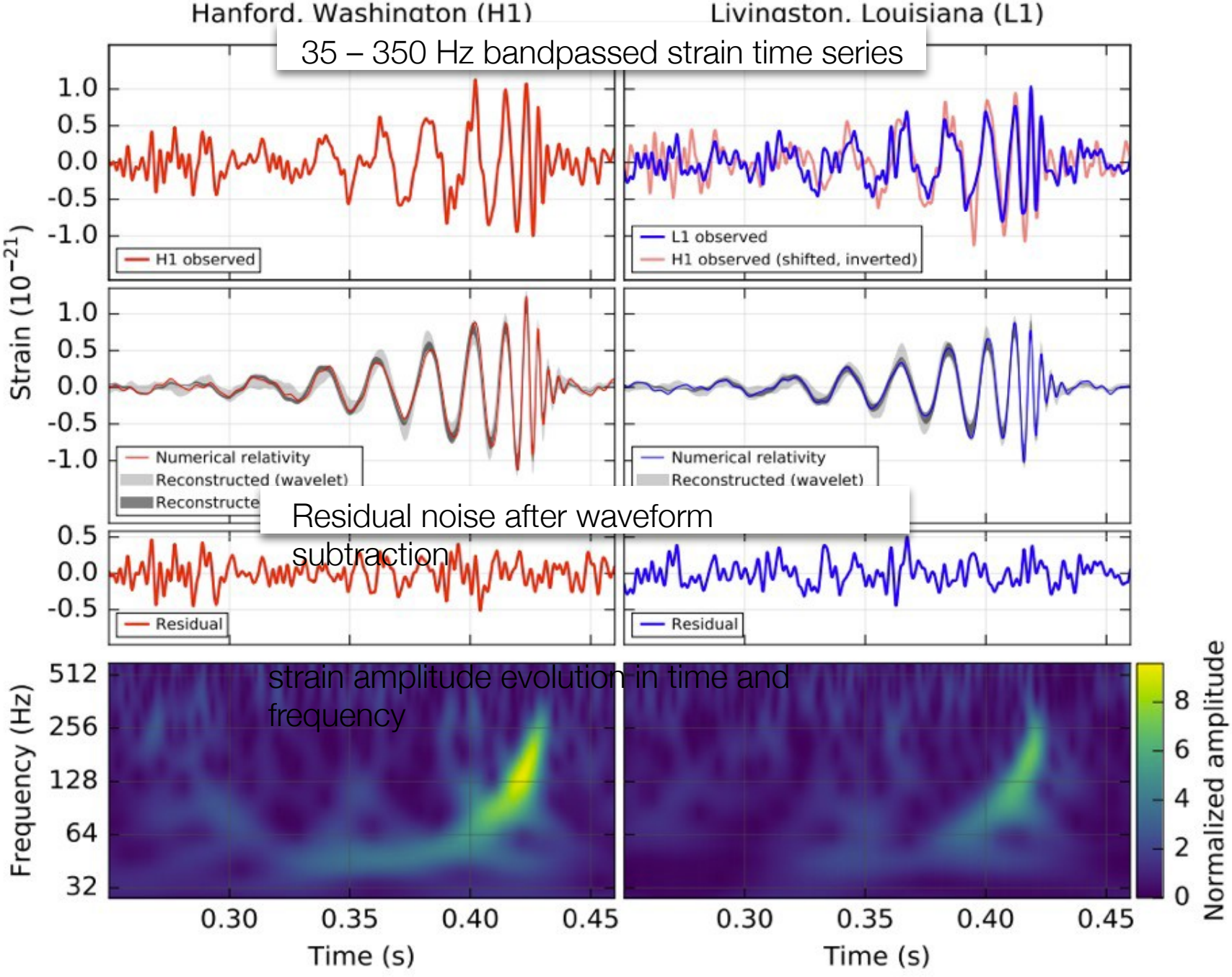
Hanford, Washington (H1)
Livingston, Louisiana (L1)
35 – 350 Hz bandpassed strain time series
Strain (10^{-21})
H1 observed
L1 observed
H1 observed (shifted, inverted)
Numerical relativity
Reconstructed (wavelet)
Residual noise after waveform subtraction
Residual
strain amplitude evolution in time and frequency
Frequency (Hz)
Time (s)
Normalized amplitude

Data Quality and Sanity Checks

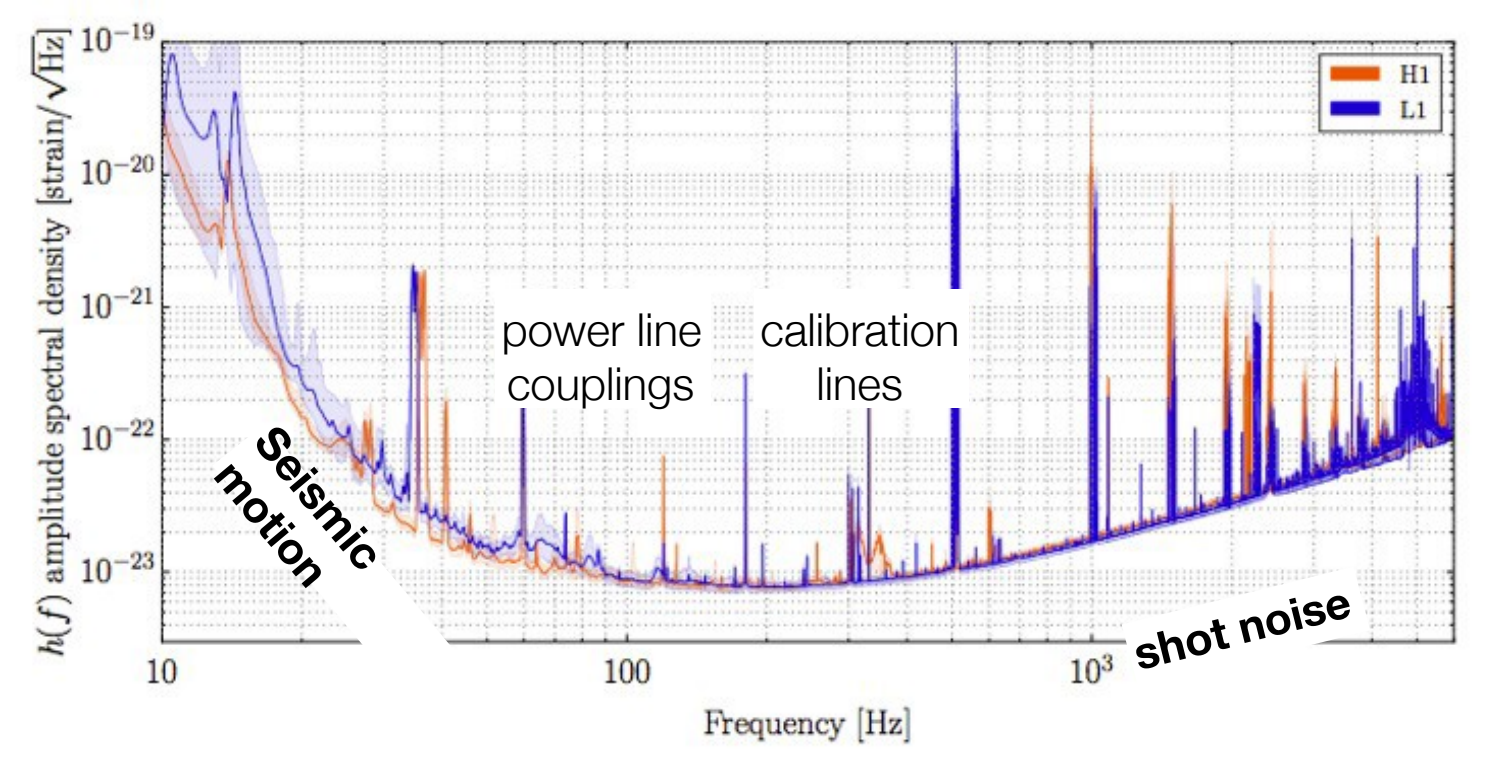

- Thousands of DAQ channels to acquire **electric, magnetic, and seismic** measurements from both instruments in addition to the cahnnels devoted to monitor nd control the status of the interferometers
- Spectral correlations as well as statistical correlations computed between transients in the channel and the GW strain channel

Data Quality and Sanity Checks

- **Candidates are vetoed if a correlation is detected**
- Data near GW150914 is **very clean**, no *a priori* or *a posteriori* vetoes would have indicated non- astrophysical origin

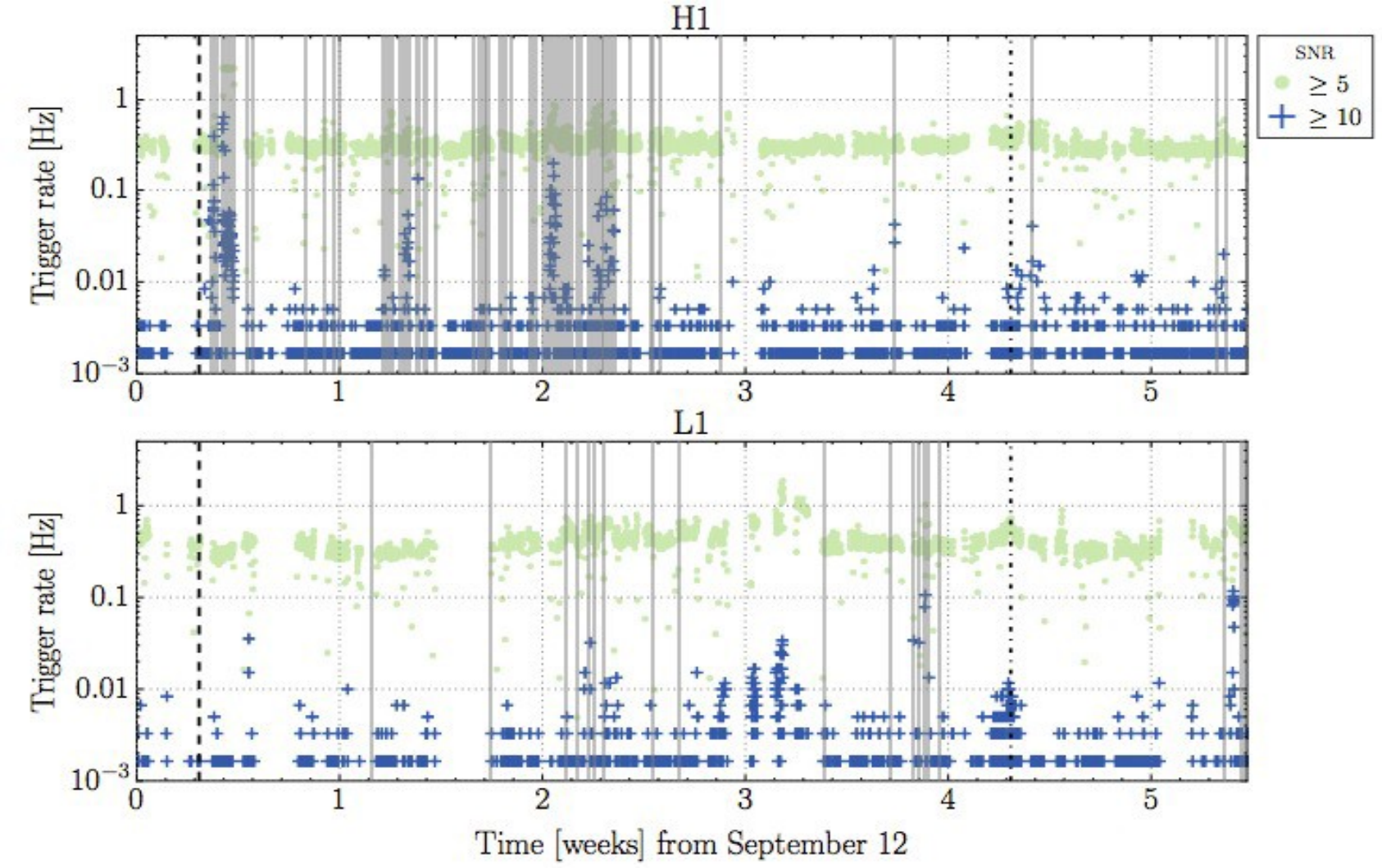

Rapid ParameterEstimation

Mass estimates and source orientation in less than an hour

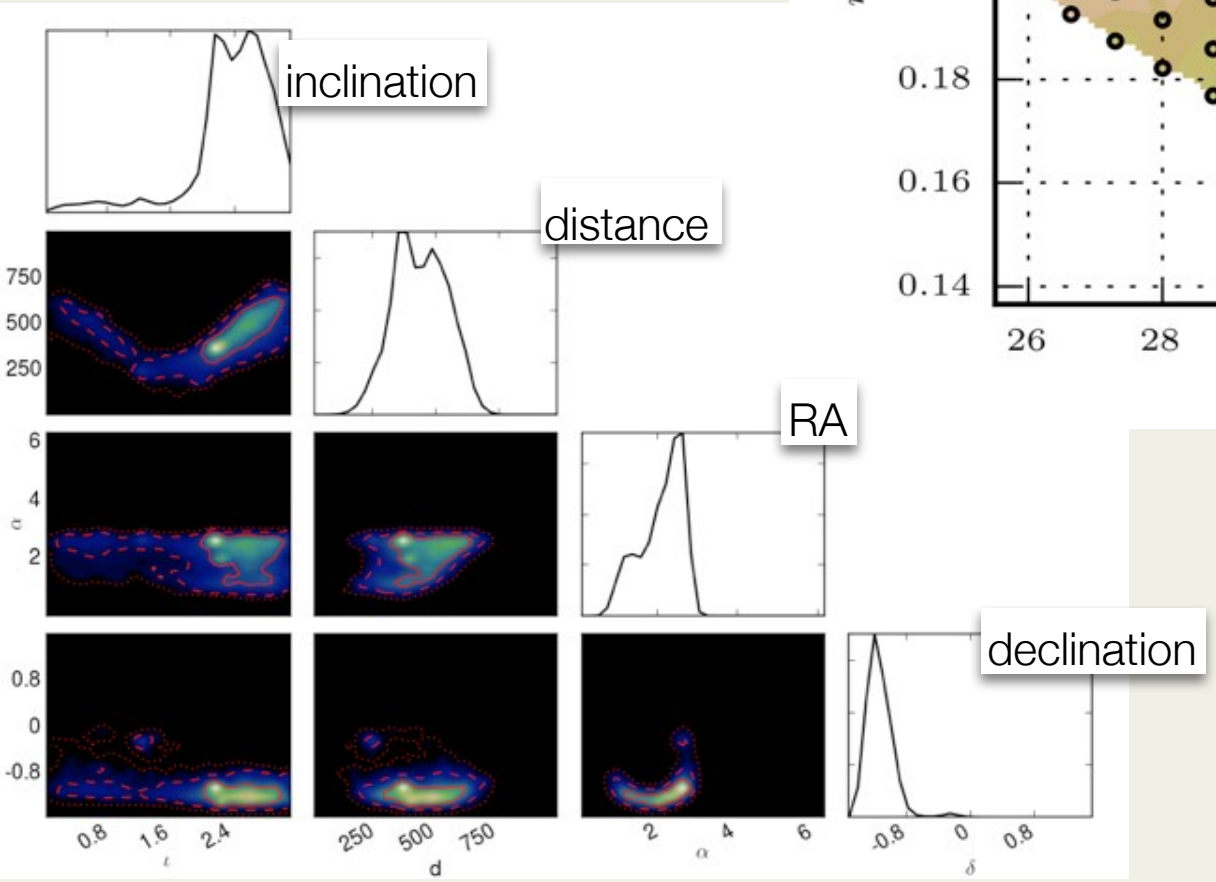

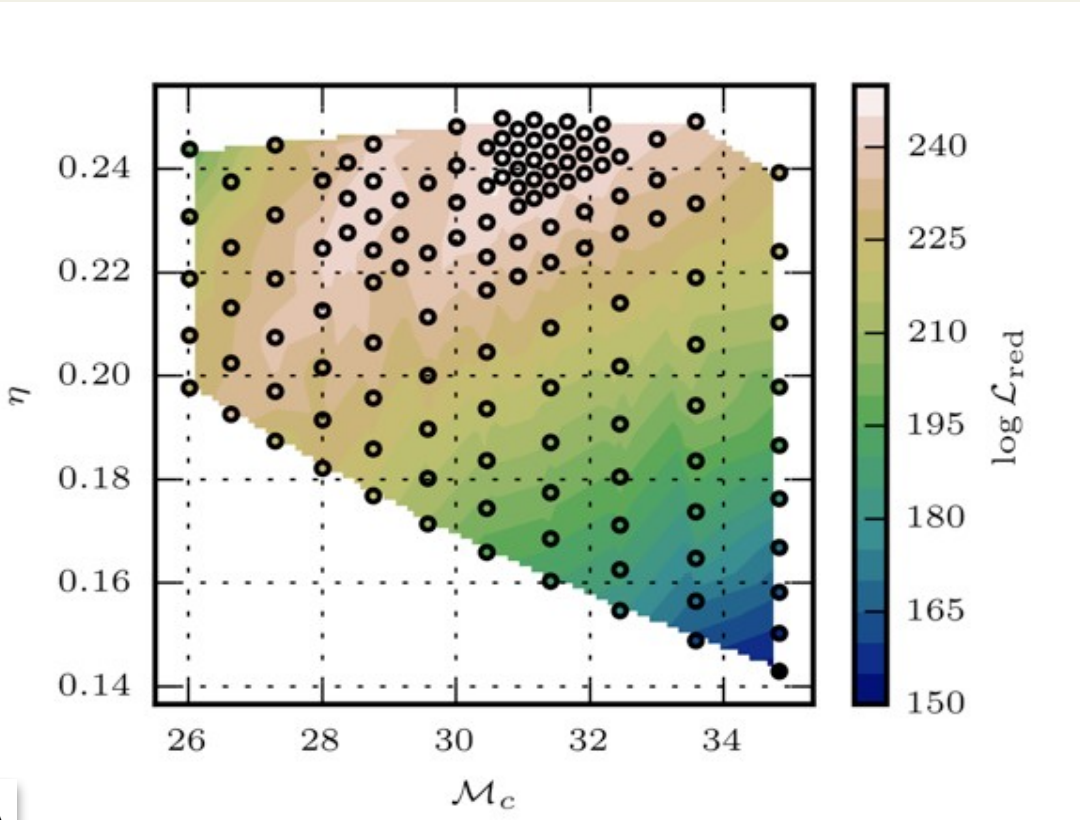

Sky areas broadly consistent with simply triangulation, and mostly cross-consistent

Triangulation ring consistent with time delay of about ~7

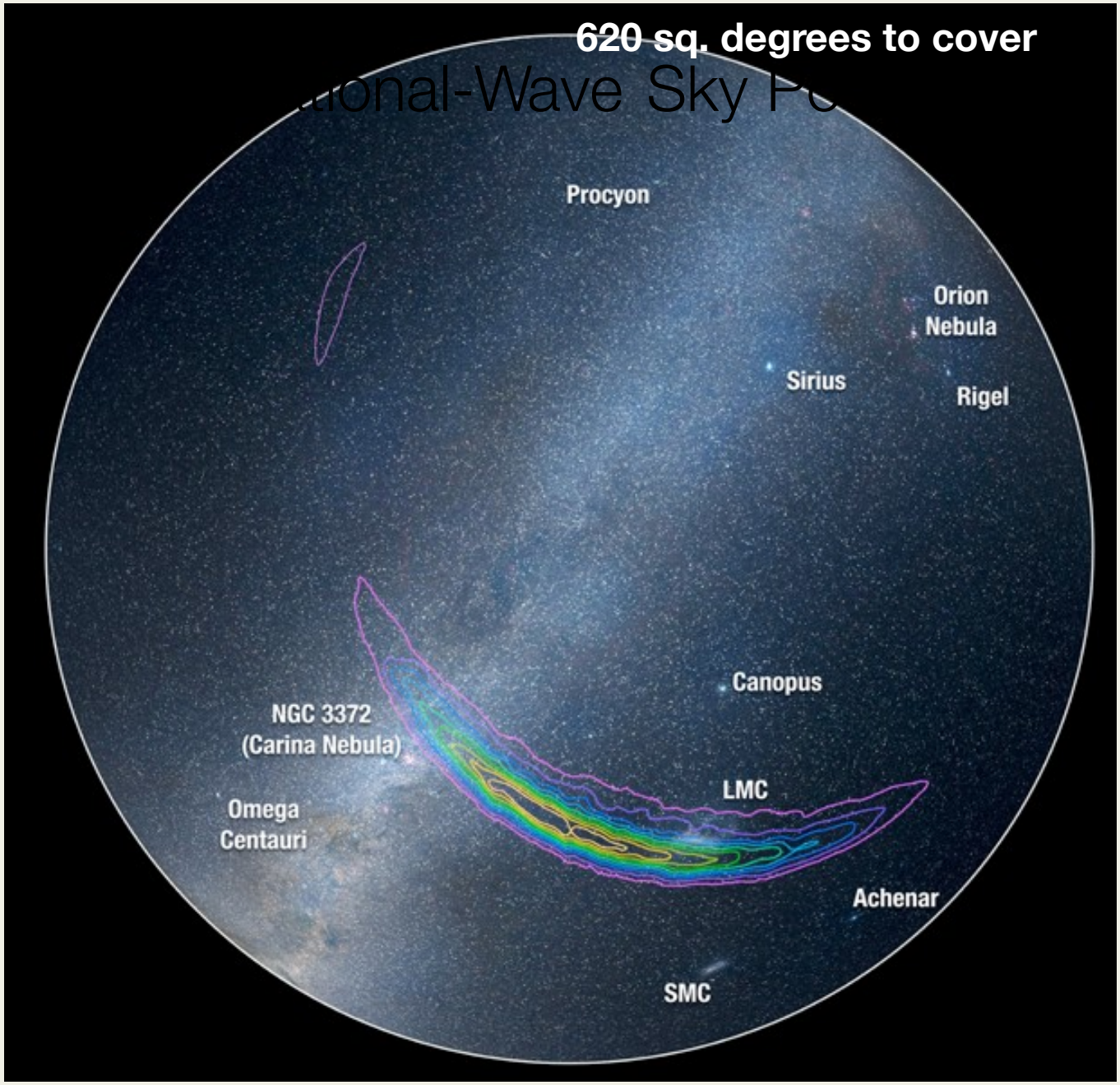

From low latency search to the offline follow-up

- Followup began immediately: given highly suggestive waveform morphology

- Markov Chain Monte Carlo methods began probing the compact binary parameter space
  - Within a day, those methods showed **very** clear confirmation: pending data quality / data calibration checks the evidence for the astrophysical origin of the signal was **overwhelming** (SNR ~24)

- Bayesian posterior probability over the sky position released to other observatories for electromagnetic facility follow up after about 48 hours

Generic transient search: minimum bias

cWB version online: event detected with 2 minutes of latency

cWB version off-line: data reanalyzed to assess the statistical significance

Events classified in 3 different classes (➔ trial factor):

- C1 class ➔ events with time-frequency morphology of known populations of noise transients: excluded;
- C3 class ➔ events with frequency that increases with time;
- C2 class ➔ all remaining events.

Background evaluation ➔ Based on the time shift method:

Number of shift produced an equivalent to 67400 years

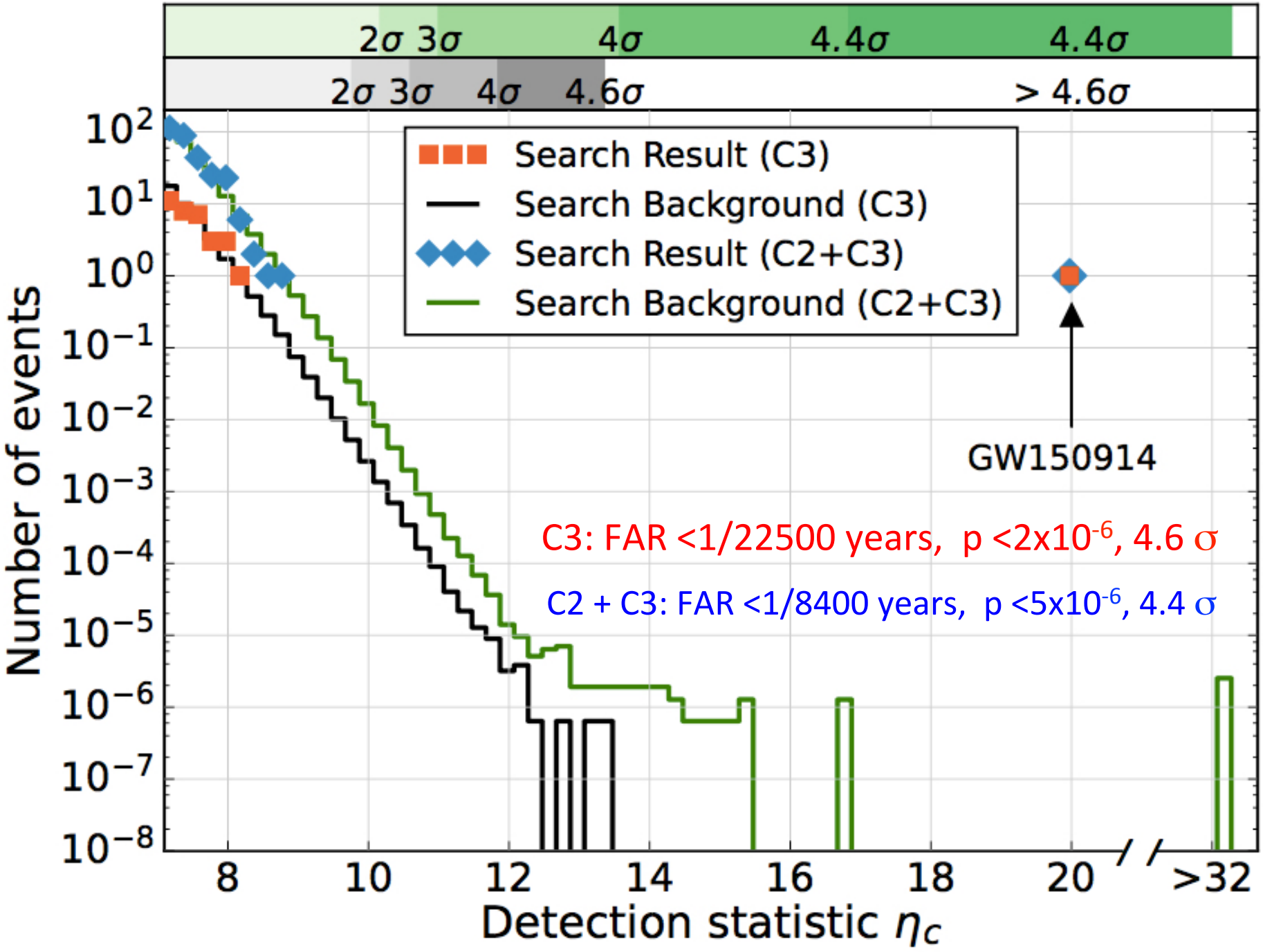
2σ 3σ 4σ 4.4σ 4.4σ
2σ 3σ 4σ 4.6σ > 4.6σ
Search Result (C3)
Search Background (C3)
Search Result (C2+C3)
Search Background (C2+C3)
GW150914
C3: FAR <1/22500 years, p <2x10-6, 4.6 σ
C2 + C3: FAR <1/8400 years, p <5x10-6, 4.4 σ
Number of events
Detection statistic η_c
10^2
10^1
10^0
10^-1
10^-2
10^-3
10^-4
10^-5
10^-6
10^-7
10^-8
8
10
12
14
16
18
20
>32

Binary Coalescence search

- 2.5 x 10^5 waveforms (mass range 1- 99 $M_\odot$)
  - EOBNR ➔ The effective-one-body (EOB) formalism combines perturbative results from the weak-field PN approximation with strong-field effects from the test-particle limit.
  - IMR-Phenomen ➔ It is based on extending frequency-domain PN expressions and hybridizing PN and EOB with NR waveforms.
- SNR of the Matched filter computed as function of time $\rho(t)$ and identify maxima and calculate χ^2 to test consistency with the matched template, then apply detector coincidence within 15 ms
- Calculate quadrature sum $\rho_C^2(t) = \rho_H^2(t) + \rho_L^2(t)$ of the SNR of each detector
- Background computed by shifting 10^7 times equivalent to 608,000 years

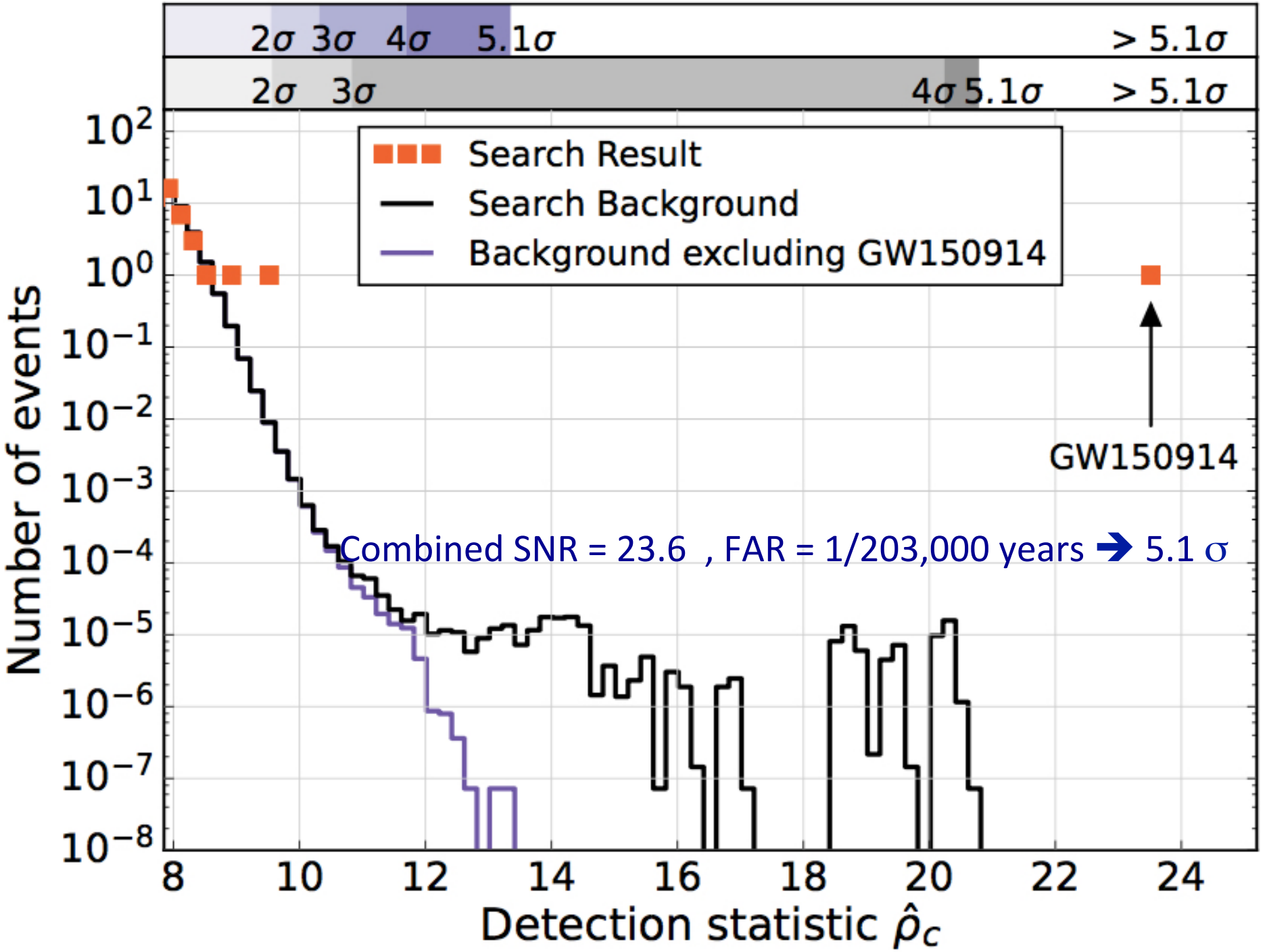
2σ 3σ 4σ 5.1σ > 5.1σ
2σ 3σ 4σ 5.1σ > 5.1σ
Search Result
Search Background
Background excluding GW150914
GW150914
Combined SNR = 23.6 , FAR = 1/203,000 years ➔ 5.1 σ
Number of events
Detection statistic $\hat{\rho}_c$

The GW 151012 case

Event much less significant!

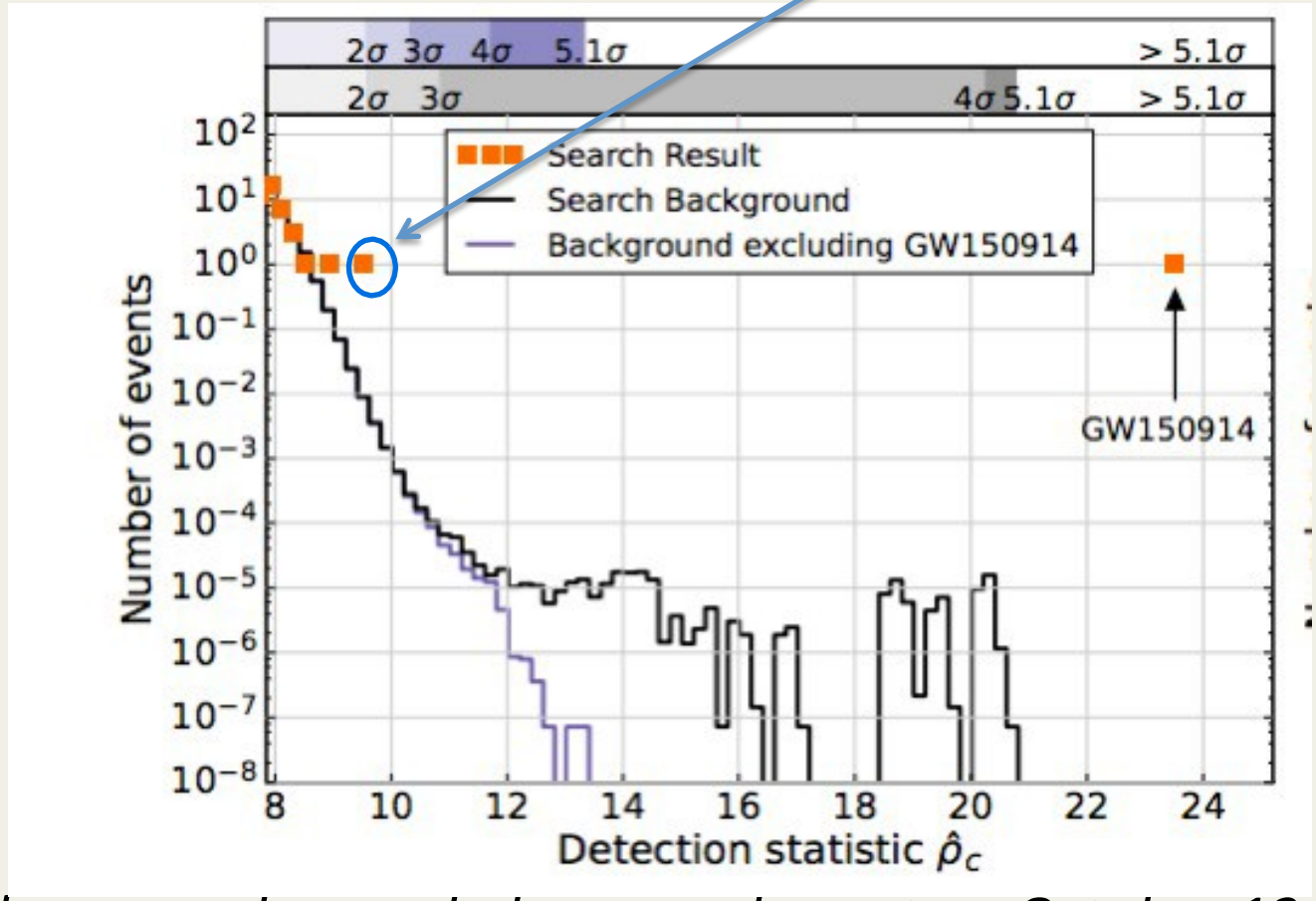

- *Full offline deep search revealed a second event on October 12, 2015: false alarm probability of ~2%*
- lif it is interpreted as a candidate of astrophysical origin, still very likely a binary black hole coalescence

Parameter Estimation

Primary black hole mass	$36^{+5}_{-4}\,\mathrm{M}_\odot$
Secondary black hole mass	$29^{+4}_{-4}\,\mathrm{M}_\odot$
Final black hole mass	$62^{+4}_{-4}\,\mathrm{M}_\odot$
Final black hole spin	$0.67^{+0.05}_{-0.07}$
Luminosity distance	410^{+160}_{-180} Mpc
Source redshift, z	$0.09^{+0.03}_{-0.04}$

One of the most energetic astronomical event ever observed:

Power emitted **~ 200 $M_\odot$ /s**

Energy emitted **~10^{49} J ➔ 3 $M_\odot c^2$**

50 times brighter of the entire visible universe

PDF- Source Distance and Orientation

Typical distance / inclination degeneracy could be broken by spin effects, now favouring a “face on” orientation

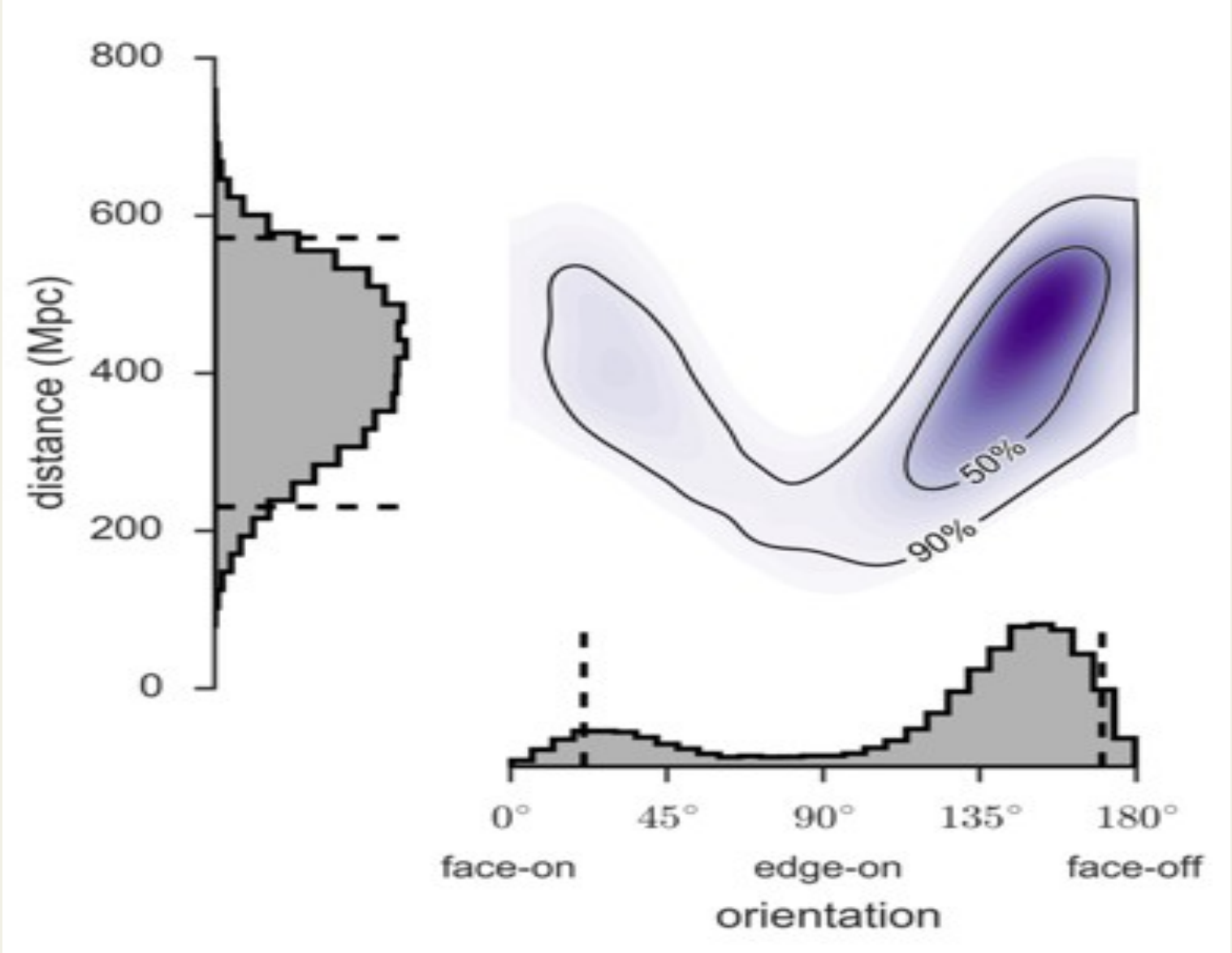

PDF - Black Hole Masses

- Degeneracies in waveform morphology arise along equal chirp mass lines in m_1/ m_2 space
- Since M_c (or total mass) is the better measured quantity m_1/m_2 is anticorrelated
- Detected masses are redshifted, lower frequency (detector frame masses are ~39 + 32 $M_\odot$)

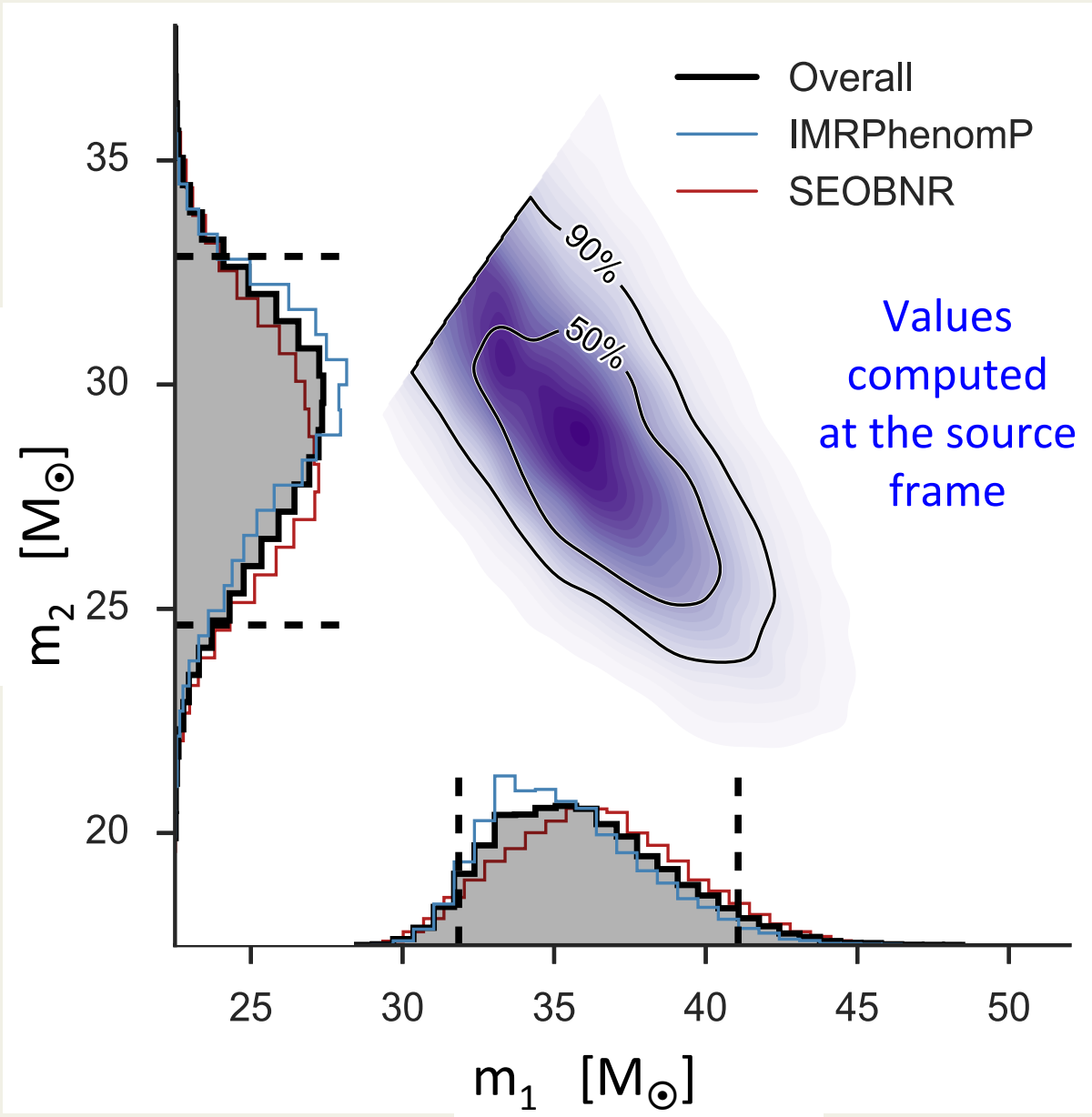

PDF - Source Spin Parameters

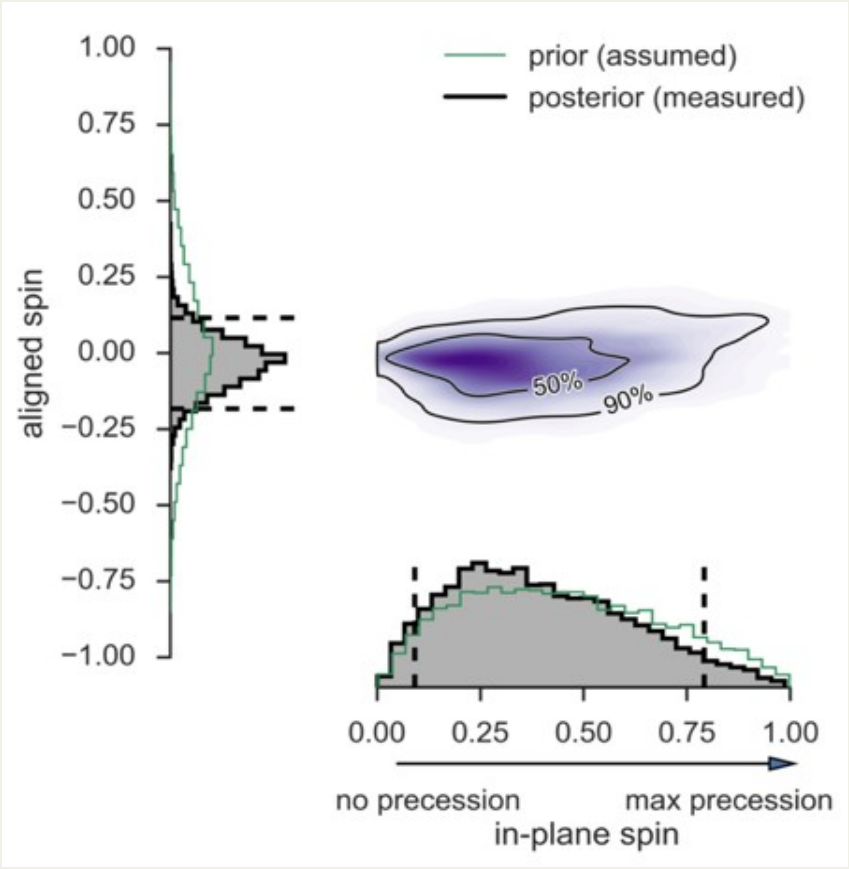

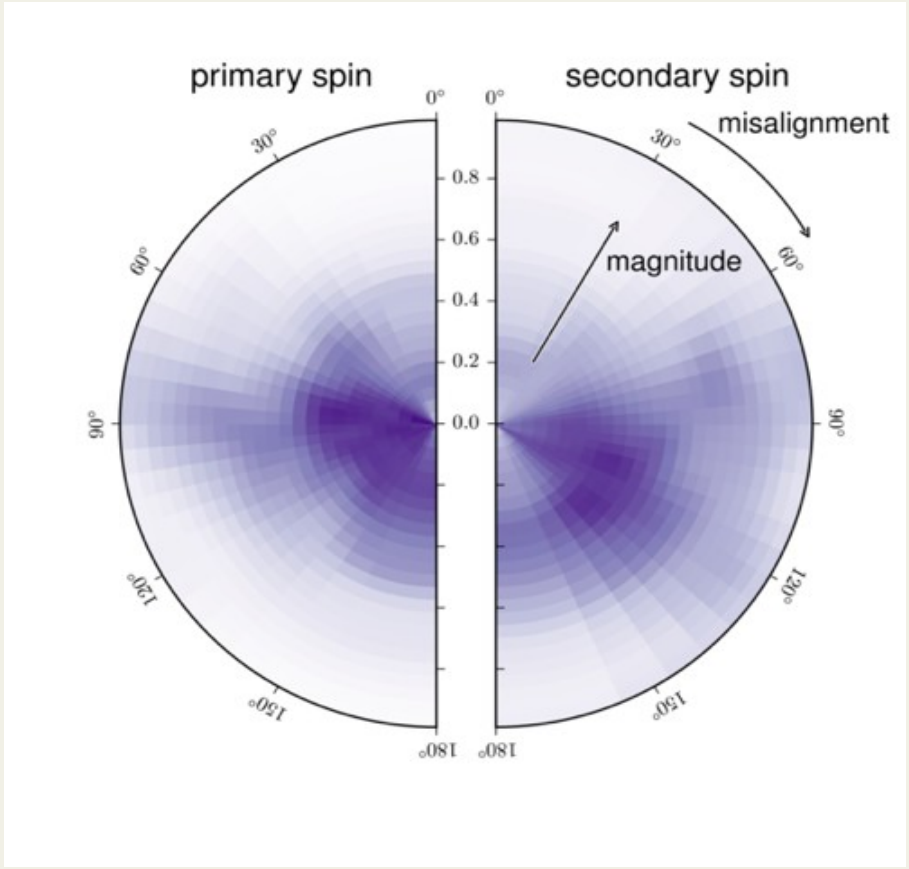

Aligned spin measures components of $S_{1,2}$ along the orbital angular momentum

Components of $S_{1,2}$ spin in the plane of the instantaneous orbit

Spin nearly aligned , but not really able to measure the precessional component

Caveat: If ***L*** aligned with line of sight (“face on”), precession is mostly unobservable

Astrophysical Event Rate

- Weak BBH formation scenarios, simulations mainly based on stellar evolution modeling

  - If you use only GW150914 (FAP ~4 x 10^{-7}): the range of rates for a "class of even with astrophysical features like this one" is

    2-53 $Gpc^{-3}\,yr^{-1}$ (median 14)

  - If you use both events (LVT151012 FAP ~0.02): the rate range for BBHs "including these two classes" is

    6 - 400 $Gpc^{-3}\,yr^{-1}$

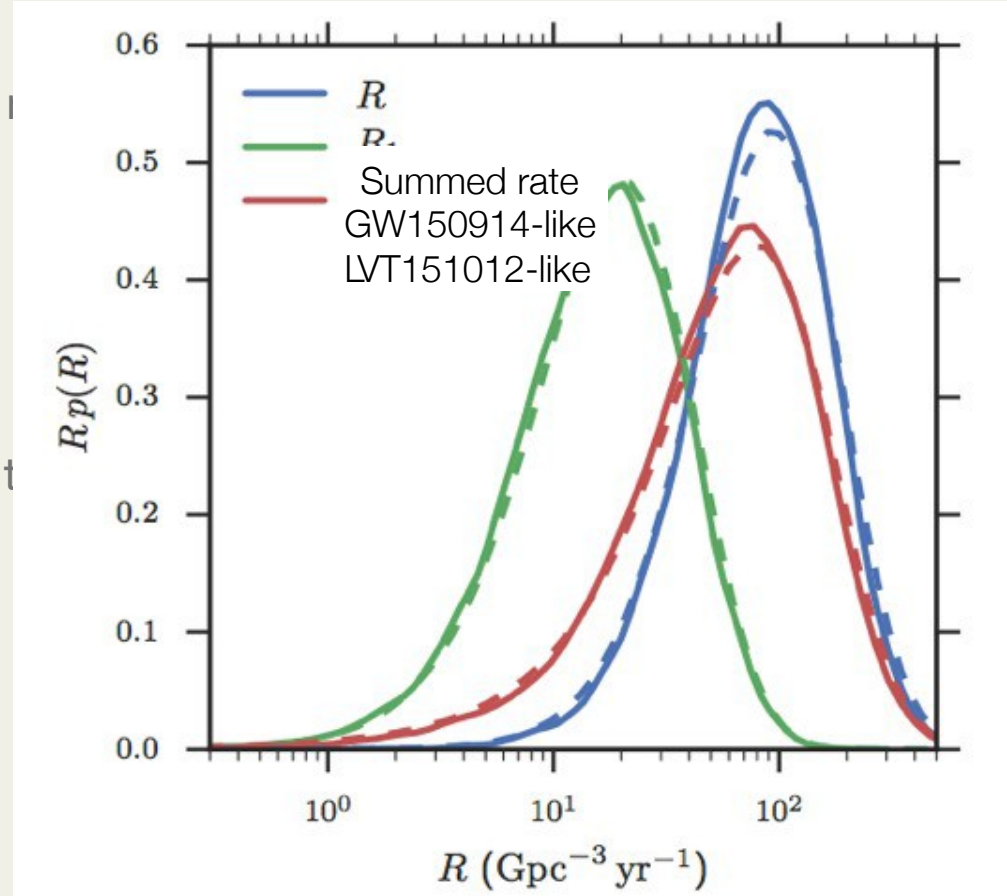

Previous rate limits (2009-2010 LIGO-Virgo run)
≤ 330 $Gpc^{-3}yr^{-1}$ (all BBH) ≤ 420 (GW150914)

Future Observational Run Rate Constraints

- Translated to detection rates for similar "loudness" (convolve those numbers with our reach and observation time): ~ 1 / 16 days

- O2 may see ~10 of GW150914 like events depending on increase in sensitivity and duration of run

- O3 may see more than 35..

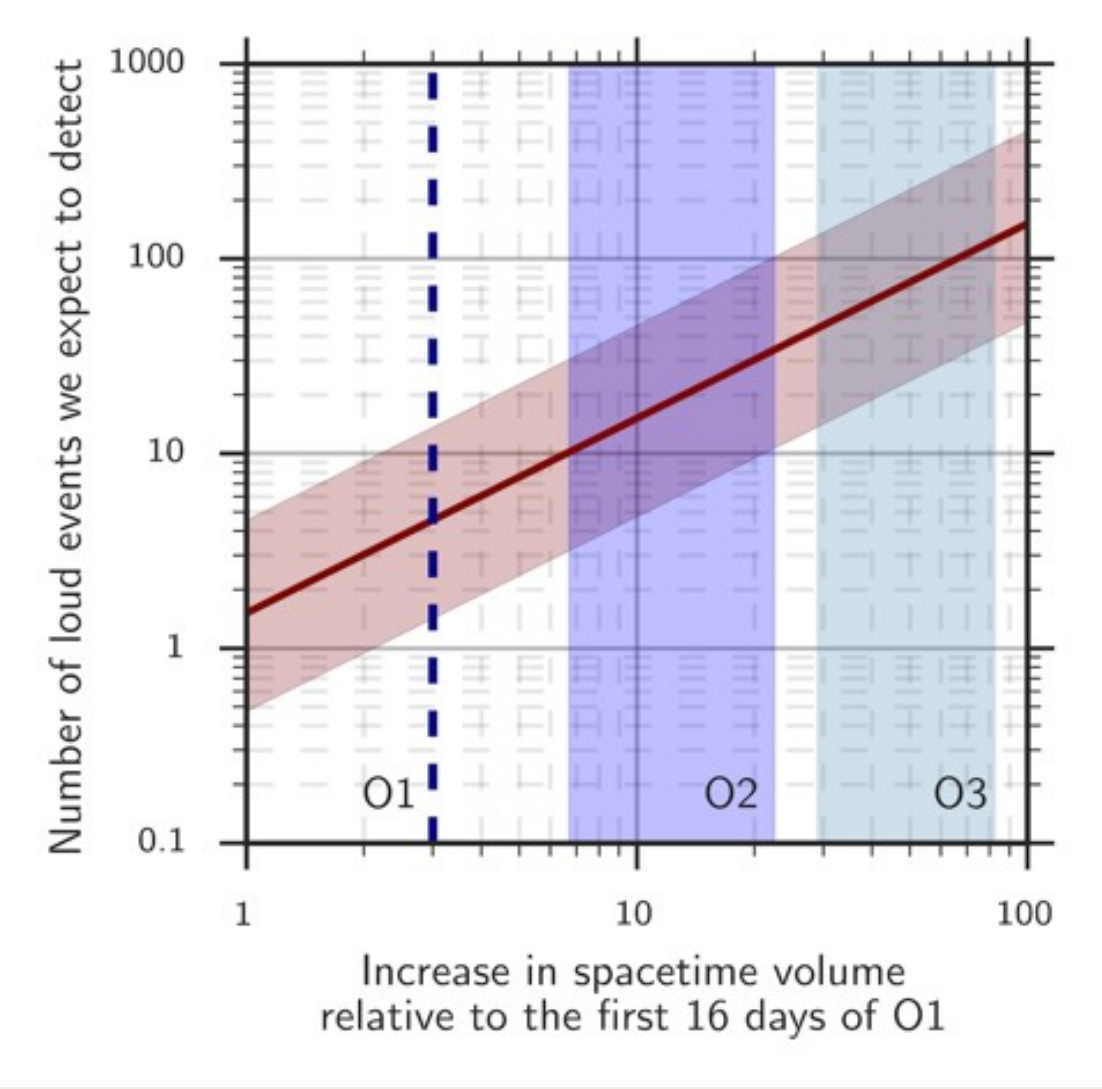

Testing General Relativity in the Strong Field regime

High v/c at merger strong field dynamics.

- Other theories predict:
  - massive graviton (e.g. $v_{grav} < c$ and dispersion effects) — **best *dynamical* constraint yet measured**
  - parameterized deviations from GR included in waveform dynamics — **not observed with significance**
- ***Present limit:***
  - ***Just one event of short duration and limited bandwidth of signal***

Testing GR: Residuals studies

- First test: how good is the "best-fit" waveform from GR?
  - Test: subtract the best-fit (estimated from MCMC studies) from the data and test the assumption that the residuals are Gaussian distributed

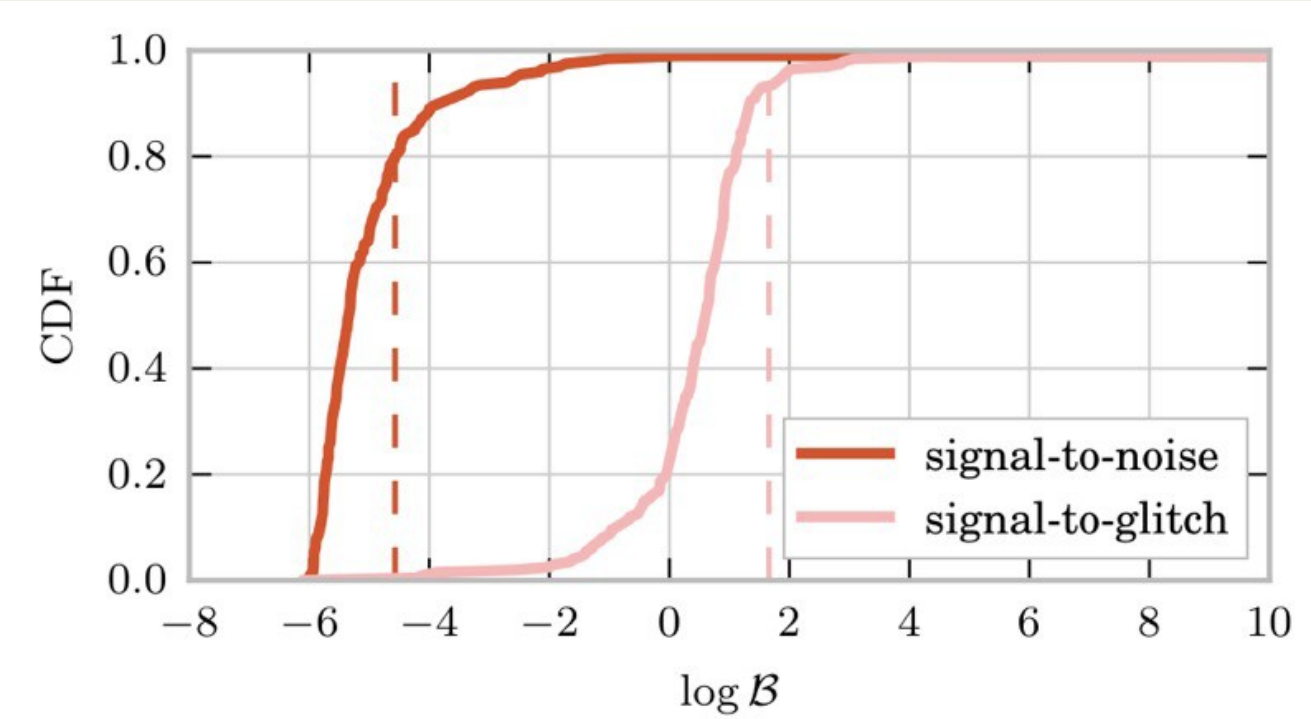

Residuals are Gaussian distributed

Residual are not Gaussian distributed but incoherent bewtween the two detectors

$\mathcal{B}$ is the ratio between the affirmative hypothesis to the negative hypothesis

Testing GR: Final mass, Spin

Check if the measured masses match with the inferred one from ring down portion

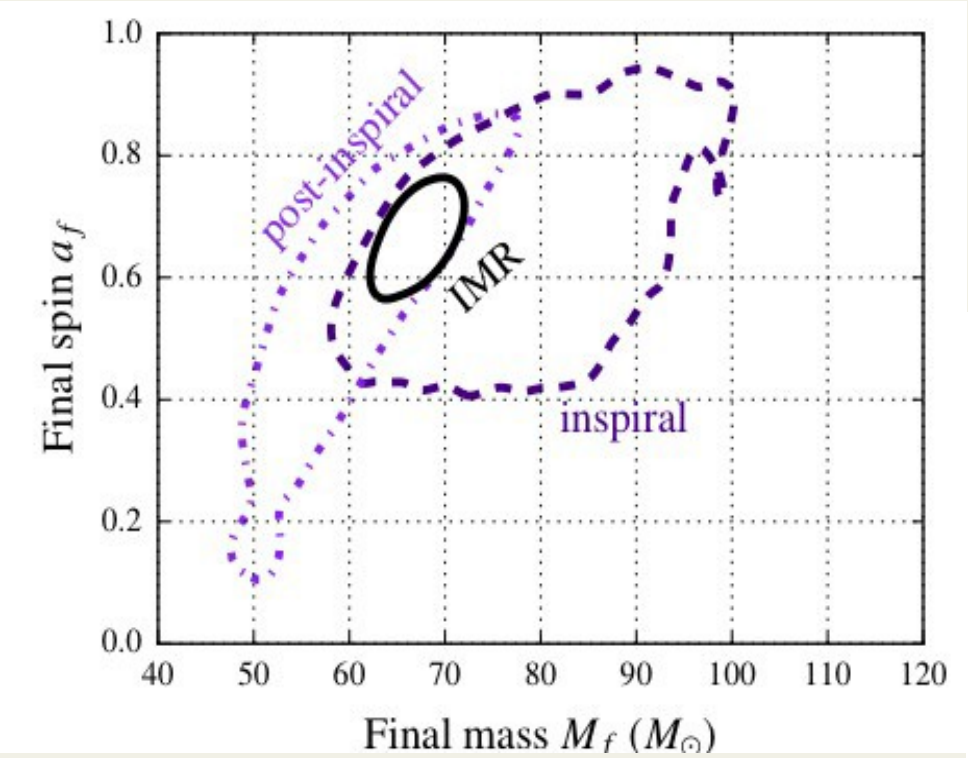

90% confidence contours on probability distributions for pre and post inspiral portions

Divide waveform into portion below and above 132 Hz (red line)

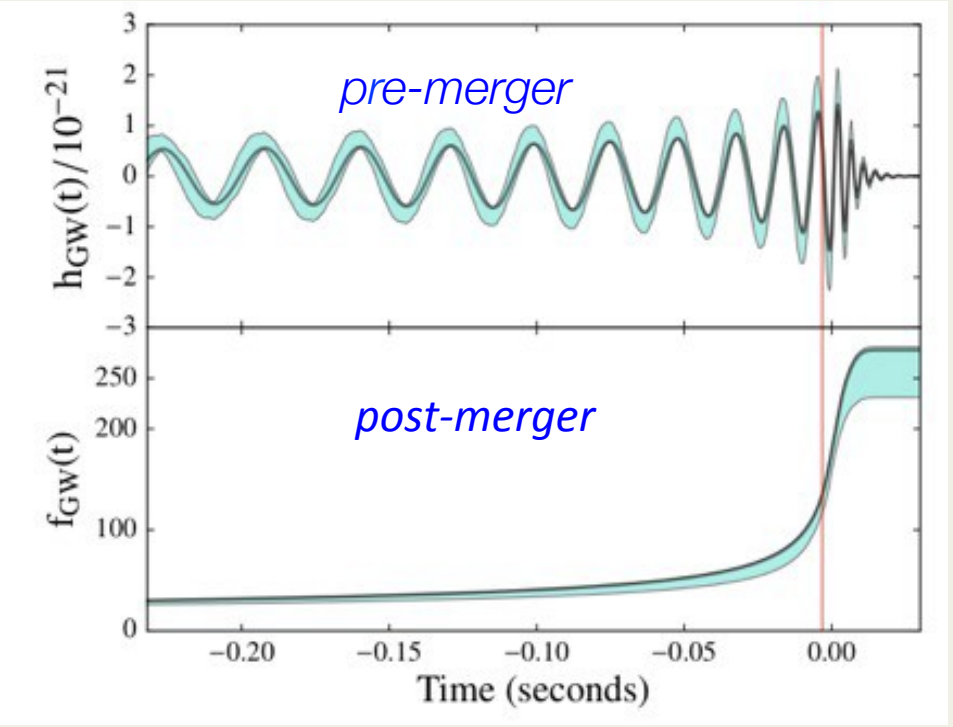

Testing GR: deviation from GR predictions

- Performed a null-hypothesis test by comparing GW150914 with a *generalized*, analytical inspiral–merger–ringdown waveform model (gIMR), which includes parameterized deformations with respect to GR
- The test is based on the computation of

  δp_i ➔ *fractional changes* in any of the parameters p_i that parameterize the GW phase expression in the baseline waveform model. These are categorized depending on which part of the wveform is considered

  - $\delta\varphi_j$, *j=0..7 phase coefficients of the early-inspiral stage*
  - σ_j , *j=0..4 phase coefficients of the late-inspiral stage*
  - β_j , *j=3,4 phase coefficients of the intermediate regime*
  - α_j , *j=2,3,4 phase coefficients of the merger-ringdown*

Testing GR: Parameterized Deviations

- "The single-parameter analysis corresponds to minimally extended models, that can capture deviations from GR that predominantly, but not only, occur at a specific PN order" — multiple-parameter analysis is highly covariant and much harder to make definitive statements

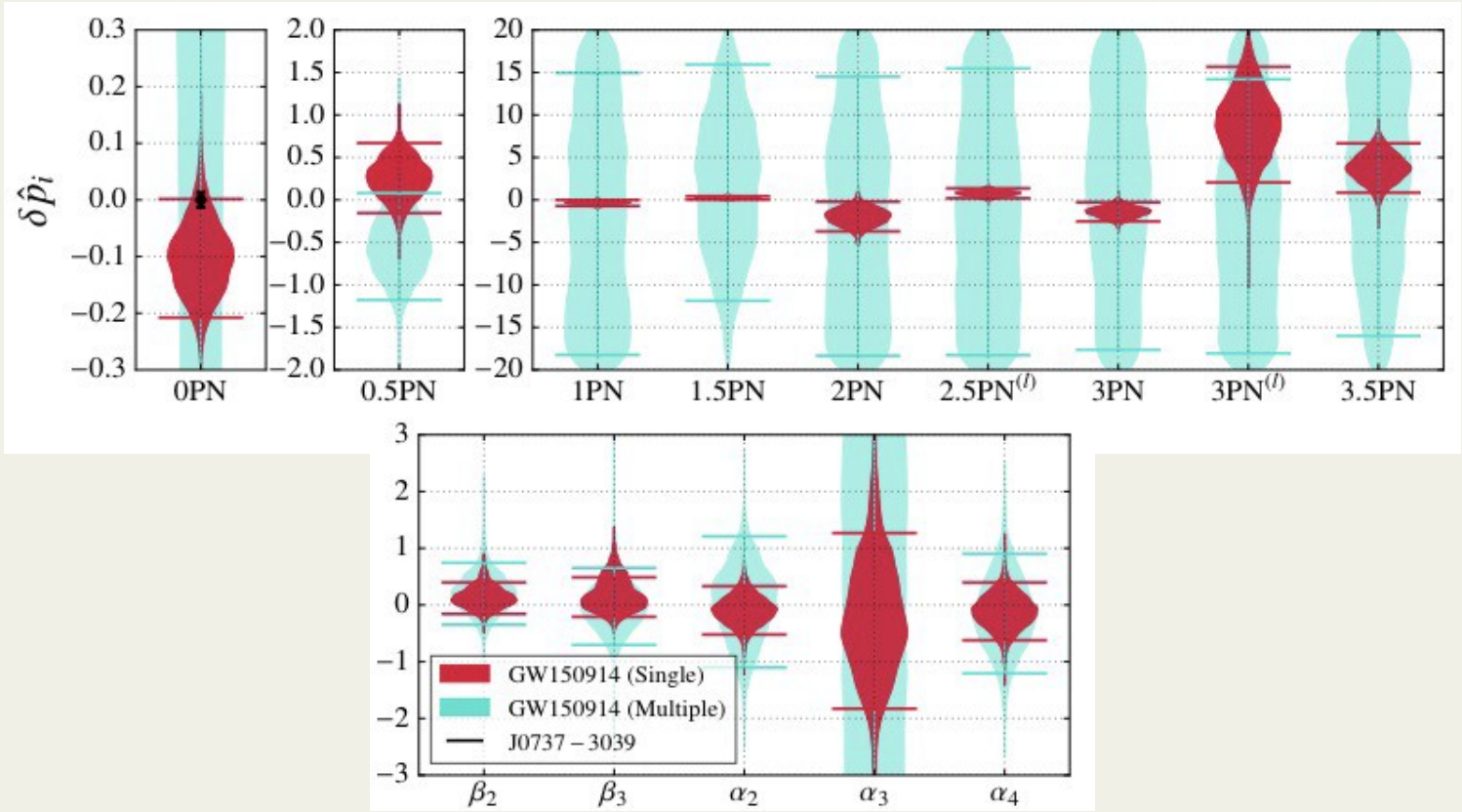

Testing GR: Massive Graviton

- Gravitons having mass indicate travel times less than the speed of light, and introduce ***dispersion***: different frequencies travel at different speed

$$\left(\frac{v}{c}\right)^2 = 1 - \left(\frac{hc}{\lambda_g E}\right)^2$$

  - λ_g is the Compton wavelength for a graviton with mass m_g — the overall effect is to "compress" the waveform in time

Our bound: $\lambda_g > 10^{13}$ *km*

- **Dynamical limits** — binary pulsar limit: $\lambda_g > 1.6 \times 10^{10}$ *km*
- Still does not exceed **limit** of 10^{22} *km* from weak lensing

A Stochastic Background from BBH

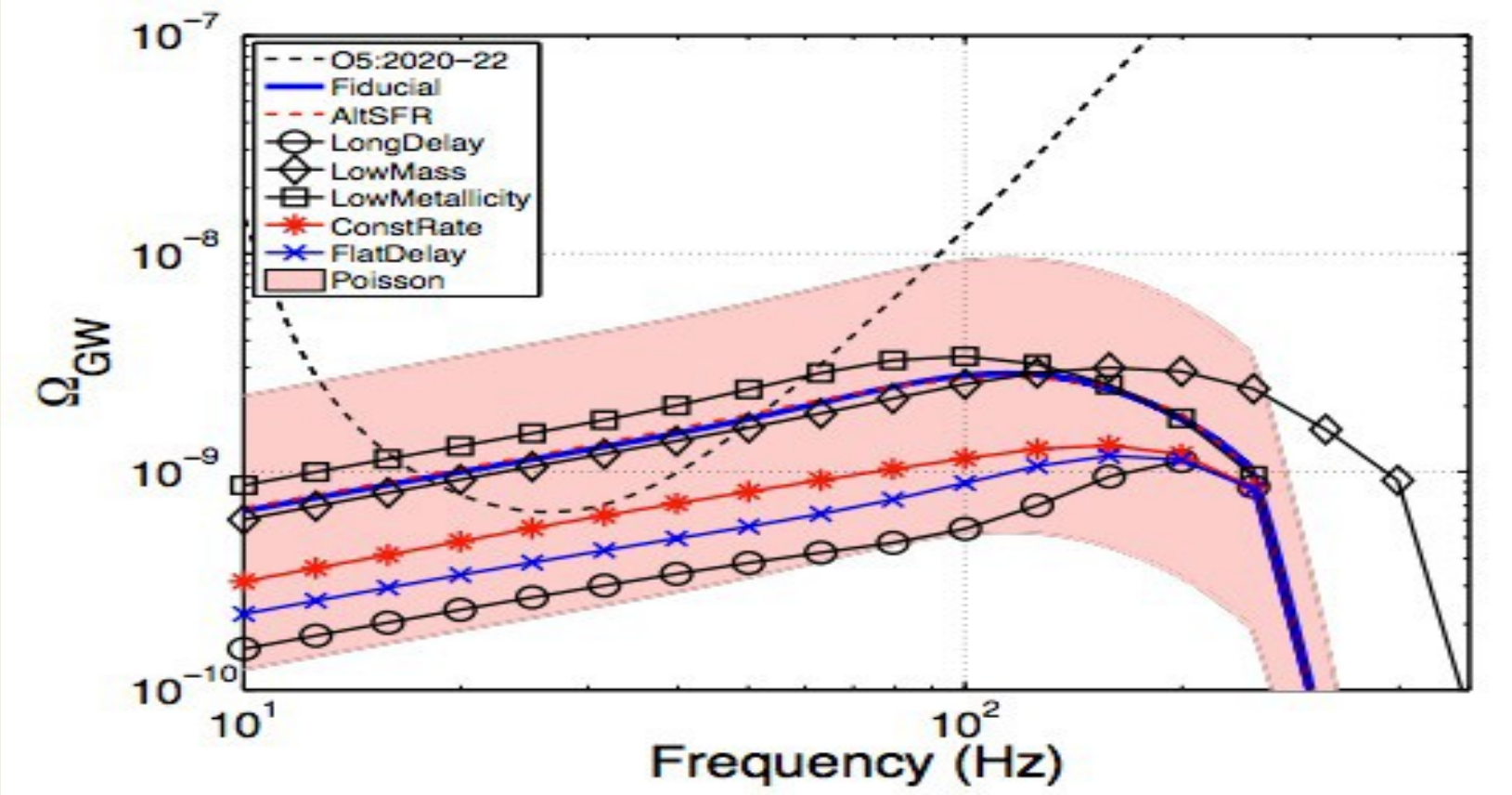

- Various models have nearly the same spectral shapes, only amplitude of the density changes... strong detection probably not achievable in next five years unless we have the high end of the source rates

$$\Omega_{\rm GW}(f;\theta_k) = \frac{f}{\rho_c H_0}\int_0^{z_{\rm max}} \frac{dz}{1+z}\frac{R_m(z,\theta_k)\left(\frac{dE(f,\theta_k)}{df}\right)_{\rm source}}{\sqrt{\Omega_M(1+z)^3+\Omega_\Lambda}}$$

Conclusion: what next?

- Virgo will join the observation
- Better sky localisation, decreased uncertainty in posterior distributions
- **New BBH events(few per week ?)**
  Hope for NSBH, BNS, SN events

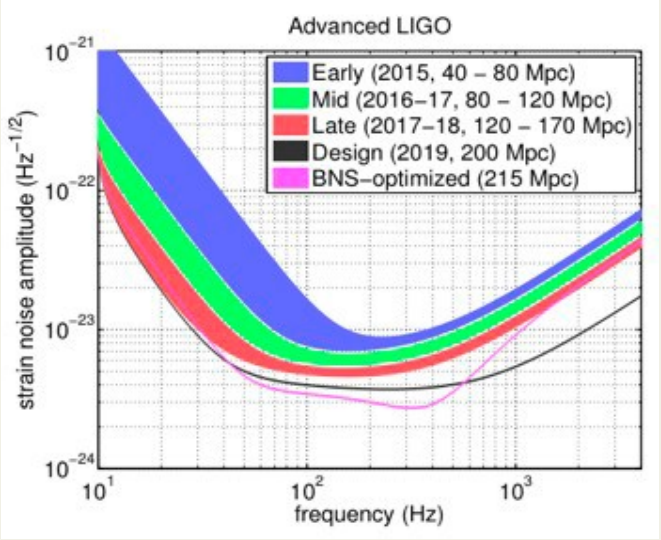

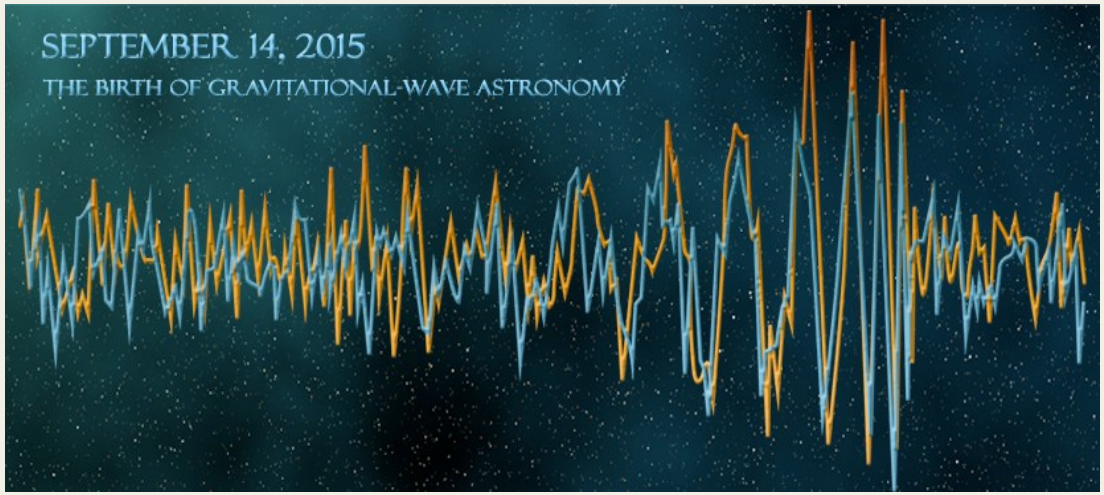

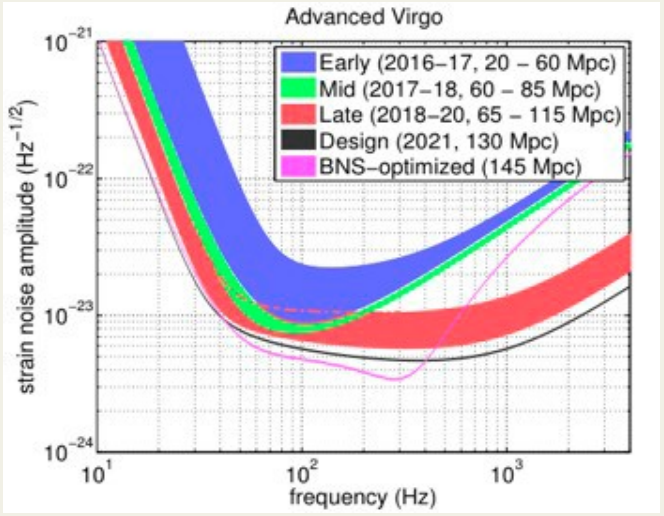

Future targets of adv. detector sensitivity

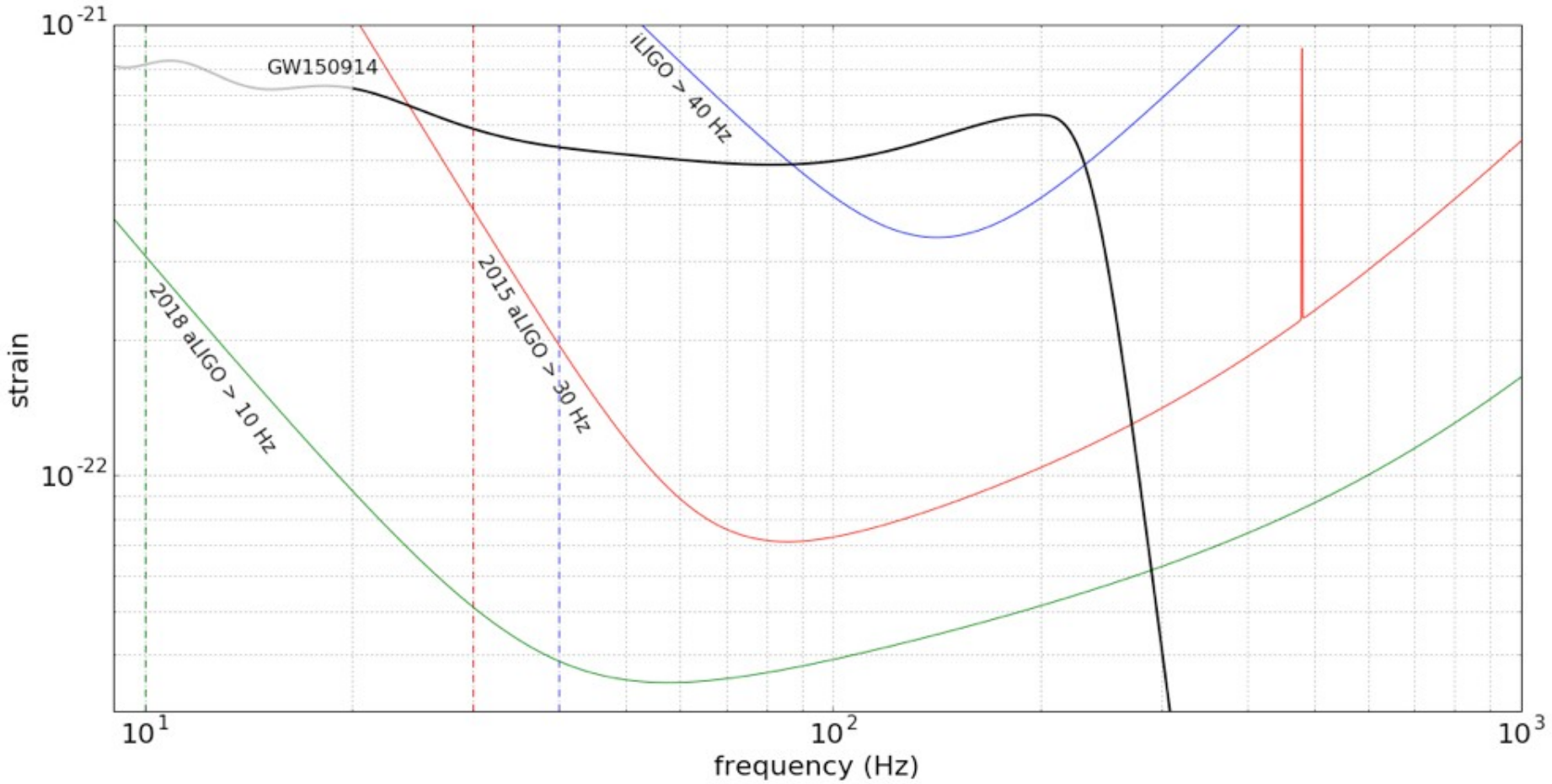

Extra Slides